NASA Contractor Report 195000

ICASE Report No. 94-84

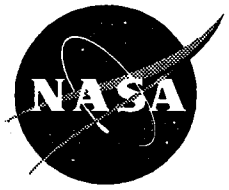

ICASE

A GENUINELY MULTIDIMENSIONAL UPWIND SCHEME AND EFFICIENT MULTIGRID SOVLER FOR THE COMPRESSIBLE EULER EQUATIONS

David Sidilkover

Contract NAS1-19480
November 1994

Institute for Computer Applications in Science and Engineering
NASA Langley Research Center
Hampton, VA 23681-0001

Operated by Universities Space Research Association

A GENUINELY MULTIDIMENSIONAL UPWIND SCHEME AND EFFICIENT MULTIGRID SOLVER FOR THE COMPRESSIBLE EULER EQUATIONS*

DAVID SIDILKOVER
ICASE, MAIL STOP 132C
NASA LANGLEY RESEARCH CENTER
HAMPTON, VA 23681

Abstract

We present a new approach towards the construction of a genuinely multidimensional high-resolution scheme for computing steady-state solutions of the Euler equations of gas dynamics. The unique advantage of this approach is that the Gauss-Seidel relaxation is stable when applied directly to the high-resolution discrete equations, thus allowing us to construct a very efficient and simple multigrid steady-state solver. This is the only high-resolution scheme known to us that has this property. The two-dimensional scheme is presented in detail. It is formulated on triangular (structured and unstructured) meshes and can be interpreted as a genuinely two-dimensional extension of the Roe scheme. The quality of the solutions obtained using this scheme and the performance of the multigrid algorithm are illustrated by the numerical experiments. Construction of the three-dimensional scheme is outlined briefly as well.

*This research was supported by DOE grant DE-FG02-92ER25139 while the author was in residence' at Courant Institute of Mathematical Sciences, 251 Mercer St., New York University, New York, NY 10012. It was also supported in part by the National Aeronautics and Space Administration under NASA Contract No. NAS1-19480 while the author was in residence at the Institute for Computer Applications in Science and Engineering (ICASE), NASA Langley Research Center, Hampton, VA 23681.

1. Introduction. A need for a fast and accurate steady-state compressible flow solver exists in many areas of science and engineering. Such a need is particularly acute for the problem of aerodynamic design. In this case steady-state solutions of the compressible flow past bodies have to be computed repeatedly, each time with variations in the body's geometry. This allows us to find the shape with optimal aerodynamic parameters relying on computations only. Thus the necessity of costly wind-tunnel experiments can be largely reduced.

The search for genuinely multidimensional schemes for the compressible Euler equations was motivated by the expectation that they will provide new possibilities (compared to the dimensionally split schemes in common use now), like:

- capturing physics of the fluid flow more accurately;
- constructing a more efficient steady-state (multigrid) solver.

Considerations regarding the first point can be found in [14],[15]. The main motivation for constructing the truly multidimensional scheme in this work is the improvement of multigrid efficiency. It was observed in [20] that pointwise Gauss-Seidel relaxation is unstable when applied directly to the high-resolution dimensionally split scheme even in the simple case of a two-dimensional scalar advection equation. Therefore, the steady-state Euler solver constructed in [21] relies on the defect correction technique, which is not a fully efficient way to utilize multigrid methods. Another possibility to avoid this difficulty is to use a multigrid algorithm that employs a well-known multi-stage Runge-Kutta relaxation technique which was developed in [9],[7],[8].

However, any further improvement of the multigrid efficiency requires us to address this problem directly: it is necessary to develop a new high-resolution (at least at the steady-state) discrete scheme, such that Gauss-Seidel relaxation is stable when applied directly to the resulting discrete equations. This was the main motivation for constructing the genuinely two-dimensional advection scheme in the control volume context in [17],[18]. The novel feature of this scheme was the two-dimensional limiter, i.e. the limiter function that relies on the ratio of two finite differences in *different* directions.

There has also been developed another class of genuinely two-dimensional advection schemes – the so-called "fluctuation-splitting" schemes. (see [6],[22]). These schemes are also equipped with a certain nonlinear mechanism that allows to combine high-resolution and a positivity properties. Several variants of such a nonlinear mechanism were devised using some geometric considerations. The remarkable feature of this approach is the simplicity of the schemes formulated on unstructured triangular grids.

The strong relationship between the fluctuation-splitting and control volume advection schemes was established in [19]. As a result, the fluctuation-splitting scheme utilizing two-dimensional limiters was constructed. The action of such a limiter function can be given a purely algebraic interpretation.

Even though some genuinely two-dimensional advection schemes were available already several years ago, the task of extending these ideas to the systems of equations appeared to be rather difficult.

The "algebraization" of the advection scheme formulation appeared to be crucial for the purpose of this work - constructing a truly multidimensional scheme for the Euler system. The resulting scheme is capable of producing high-resolution steady-state solutions. Its unique feature is that the Gauss-Seidel relaxation is stable when applied directly to the high resolution discrete equations.

The paper is organized as follows: in §2 we give a brief introduction into the fluctuation-splitting approach for the scalar advection equations and present considerations for extending this approach to systems of equations in two dimensions. In §3 we take a closer look at the Roe scheme for the Euler equations in one dimension. Then we construct a truly two-dimensional scheme for the Euler systems on structured (in §4) and unstructured (§5) triangular grids. In §6 we outline first as a preliminary the construction of the three-dimensional advection scheme. Then we present a truly three-dimensional scheme for the Euler system. §7 describes the multigrid algorithm that employs the constructed truly two-dimensional scheme. Numerical experiments are presented in §8, followed by discussion and conclusions in §9.

2. Preliminaries and motivation. In the first part of this section we illustrate the fluctuation-splitting approach, first on the example of scalar advection in one dimension. Then we present the construction of a simple truly two-dimensional advection scheme that relies on two-dimensional limiters. In the second part we discuss the difficulties that arise when trying to apply the scalar advection schemes to discretize systems of equations in multidimensions.

2.1. Fluctuation-splitting approach. We shall give here a brief description of the fluctuation-splitting advection scheme in one and two dimensions (for details see [6],[19]). These schemes are required to have properties of *positivity* and *linearity preserving*. We shall define here the *positivity* property.

DEFINITION 2.1. *A scheme is said to be of the positive type if any solution value on the new time level obtained by this scheme can be written as a positive combination of the values from the previous time level.*

Solutions obtained by using positive schemes will satisfy a certain maximum principle and, therefore, do not exhibit oscillatory behavior in presence of discontinuities.

The notion of *linearity preserving* is used to characterize high-resolution at the steady-state schemes. It is trivial in one dimension. Therefore, we shall give its precise definition in §2.1.2.

2.1.1. Advection in one dimension. Consider a linear one-dimensional advection equation

$$u_t + a u_x = 0 \tag{1}$$

We are interested in solving it numerically on a grid with meshsize h (see Fig.1). Fluctuation is defined as the residual of the equation on the linear element multiplied by the volume of the element. In our case the fluctuation on the segment $[i-1, i]$ is defined as the residual of (1) on this segment multiplied by its length h

$$R = -a(u_i - u_{i-1})$$

The numerical solution can be interpreted as a two-stage process

- compute the fluctuation on each element and distribute (split) it among the vertices of this element;
- update the solution at each vertex due to the accumulated portions of fluctuations.

Denoting by τ the time-step and distributing the fluctuation on the segment $[i-1, i]$ equally between the adjacent gridpoints

$$hu_{i-1}^{n+1} = hu_{i-1}^{n} + \frac{\tau}{2} R + C.O.E.$$

$$hu_i^{n+1} = hu_i^n + \frac{\tau}{2}R + C.O.E.$$

we obtain the central scheme, which is neither positive nor stable, though second order accurate in space. Here "*C.O.E.*" stands for "contributions from other elements" and will be omitted in the remainder of this paper.

The upwind scheme can be obtained by adding a proper amount of the artificial viscosity to the central scheme. The fluctuation distribution formulae thus become

$$\begin{aligned} hu_{i-1}^{n+1} &= hu_{i-1}^n + \tfrac{\tau}{2}(R - \bar{R}) \\ hu_i^{n+1} &= hu_i^n + \tfrac{\tau}{2}(R + \bar{R}), \end{aligned} \tag{2}$$

where

$$\bar{R} = -|a|(u_i - u_{i-1}) = \text{sign}(a)R$$

is the artificial viscosity.

It is easy to see that in this case the entire fluctuation on the segment $[i-1, i]$ contributes to the solution update either at the left or at the right nodes of the segment depending on the advection direction (sign).

2.1.2. Two-dimensional advection. Consider a linear two-dimensional advection equation

$$u_t + au_x + bu_y = 0$$

The fluctuation on the triangle T (see Fig.2) is given by

$$R = R^x + R^y, \tag{3}$$

where

$$\begin{aligned} R^x &= -\tfrac{h}{2}[a(u_0 - u_3)] \\ R^y &= -\tfrac{h}{2}[b(u_3 - u_4)] \end{aligned}$$

Assuming that the fluctuation distribution formulae in this case are

$$\begin{aligned} h^2u_0^{n+1} &= h^2u_0^n + \tfrac{\tau}{2}(R^x + \bar{R}^x) \\ h^2u_3^{n+1} &= h^2u_3^n + \tfrac{\tau}{2}[(R^x - \bar{R}^x) + (R^y + \bar{R}^y)] \\ h^2u_4^{n+1} &= h^2u_4^n + \tfrac{\tau}{2}(R^y - \bar{R}^y) \end{aligned} \tag{4}$$

where $\bar{R}^x, \bar{R}^y$ are the artificial viscosity terms defined by

$$\begin{aligned} \bar{R}^x &= \text{sign}(a)R^x \\ \bar{R}^y &= \text{sign}(b)R^y, \end{aligned} \tag{5}$$

we obtain the dimensional upwind scheme which is *positive*, but only first order accurate.

DEFINITION 2.2. *The fluctuation-splitting scheme is called linearity preserving if whenever the fluctuation on the triangle T vanishes then the scheme leads to a zero update in each of the three vertices of the triangle.*

It was observed in [6] that linearity-preserving schemes on structured grids produce numerical solutions that are second-order accurate in the steady state.

Introduce the following quantities

$$R^{x^*} = R^x + R^y \Psi(Q)$$
$$R^{y^*} = R^y + R^x \frac{\Psi(Q)}{Q} \tag{6}$$

where

$$Q = -\frac{R^x}{R^y} \tag{7}$$

and Ψ is a Lipschitz continuous limiter function such that

$$0 \le \Psi(Q) \le 1, \quad 0 \le \frac{\Psi(Q)}{Q} \le 1 \tag{8}$$

and

$$\Psi(1) = 1 \tag{9}$$

Substituting R^{x^*}, R^{y^*} for R^x, R^y into (4) and (5) we obtain a linearity preserving (second order accurate at the steady-state in the case of structured grid) scheme. Using the following identity

$$R^y \Psi(Q) \equiv -R^x \frac{\Psi(Q)}{Q} \tag{10}$$

it is easy to see that the scheme defined by (4),(5) and (6) is of the positive type.

It is also obvious from (10) that such scheme is conservative because

$$R^{x^*} + R^{y^*} \equiv R^x + R^y \equiv R$$

(for more details see [19]).

2.2. Hyperbolic systems of equations. We shall explain here what is the main obstacle encountered when constructing a truly two-dimensional numerical scheme for a hyperbolic system of equations. We shall also describe our approach to overcoming it. An understanding of the basic differences between the one- and two-dimensional cases is required for this purpose. These differences will be illustrated on linear systems of equations.

2.2.1. One dimension. Consider a system of conservation laws in one dimension

$$\boldsymbol{u}_t + \boldsymbol{f}(\boldsymbol{u})_x = 0 \tag{11}$$

For the purpose of the discussion here it is sufficient to look at the linear constant coefficient case of (11). Consider the following system of partial differential equations

$$\boldsymbol{u}_t + A\boldsymbol{u}_x = 0 \tag{12}$$

where A is an $N \times N$ matrix. The system (12) is said to be hyperbolic if matrix A has a complete set of real eigenvalues.

Denote by T the matrix of right eigenvectors of A. Then

$$\Lambda = T^{-1} A T$$

is a diagonal matrix. Introducing *characteristic* variables

$$\boldsymbol{w} = T^{-1}\boldsymbol{u}$$

(12) can be rewritten as a set of N decoupled advection equations:

$$\boldsymbol{w}_t + \Lambda \boldsymbol{w}_x = 0. \tag{13}$$

It is clear from (13) that a one-dimensional advection scheme can be applied in a straightforward way to solve a (linear) hyperbolic system of equations in one dimension. A discussion concerning the nonlinear Euler system in one dimension will be presented in the §3.

2.2.2. Two dimensions. A linear system of partial differential equations in two dimensions of the following form

$$\boldsymbol{u}_t + A\boldsymbol{u}_x + B\boldsymbol{u}_y = 0 \tag{14}$$

is said to be hyperbolic if the matrix

$$\mathcal{A} = \cos\phi A + \sin\phi B$$

has a complete set of real eigenvalues for $\forall\phi : 0 \leq \phi \leq 2\pi$. In this case there exist matrices T_A and T_B such that $T_A^{-1}AT_A$ and $T_B^{-1}BT_B$ are diagonal. This is usually utilized to construct the so-called dimensionally split schemes.

However, matrices A and B in general do not commute. Therefore, $T_A \neq T_B$, i.e. a hyperbolic system in two dimensions cannot be represented as a set of decoupled advection equations (unlike the one-dimensional case). This means that a truly two-dimensional advection scheme cannot be applied in a straightforward way to discretize a hyperbolic systems of equations.

Much of the research effort in the last several years concentrated on finding a way to apply the multidimensional advection schemes to discretize hyperbolic systems of equations, in particular the Euler equations of gas dynamics. One of the major directions was the so-called wave modeling (see [14],[5]). This approach concentrated on finding a way to represent (locally) the physics of two-dimensional flow of a compressible fluid by a finite number of simple waves, each one having an associated advection equation.

The approach we present here is concerned not with applying an advection scheme to discretize a system of equations in two dimensions, but rather with applying to the systems of equations the same strategy that was used when constructing a scalar advection scheme. The construction of the genuinely two-dimensional scheme for the Euler will be presented in §4 for the structured grids and in §5 for the general unstructured grids case.

3. Euler equations in one dimension and Roe scheme. The Euler equations of gas dynamics in one dimension can be written as follows

$$\boldsymbol{u}_t + \boldsymbol{F}(\boldsymbol{u})_x = \mathbf{o}, \tag{15}$$

where

$$\boldsymbol{u} = \begin{pmatrix} \rho \\ \rho u \\ e \end{pmatrix}; \quad \boldsymbol{F}(\boldsymbol{u}) = \begin{pmatrix} \rho u \\ \rho u^2 + p \\ \rho u H \end{pmatrix}, \tag{16}$$

the enthalpy H is defined by

$$H = \frac{e+p}{\rho} = \frac{c^2}{\gamma - 1} + \frac{1}{2}u^2, \tag{17}$$

the speed of sound

$$c = \sqrt{\frac{\gamma p}{\rho}} \tag{18}$$

and the pressure

$$p = (\gamma - 1)(e - \frac{1}{2}\rho u^2) \tag{19}$$

The Jacobian matrix

$$\mathcal{A} = \frac{\partial \boldsymbol{F}}{\partial \boldsymbol{u}} \tag{20}$$

has real eigenvalues only.

In order to apply the upwind differencing approach to the nonlinear system (15) a particular conservative linearization procedure was introduced by Roe [13]. For two states $\boldsymbol{u}_l$ and $\boldsymbol{u}_r$ a matrix $\tilde{A}(\boldsymbol{u}_l, \boldsymbol{u}_r)$ was constructed having certain properties called together *Property U*. We address the reader to [13] for the details. Let us only mention here one of these properties: the following identity holds for any $\boldsymbol{u}_l, \boldsymbol{u}_r$:

$$\tilde{A}(\boldsymbol{u}_l, \boldsymbol{u}_r) \cdot (\boldsymbol{u}_r - \boldsymbol{u}_l) \equiv \boldsymbol{F}(\boldsymbol{u}_r) - \boldsymbol{F}(\boldsymbol{u}_l). \tag{21}$$

3.1. Fluctuation-splitting formulation. Define the fluctuation on the considered element (segment $[i-1, i]$, see Fig.1)

$$\boldsymbol{R} = -[\boldsymbol{F}(\boldsymbol{u}_i) - \boldsymbol{F}(\boldsymbol{u}_{i-1})]. \tag{22}$$

Following the Roe-linearization procedure we assume that the quantities which vary linearly on the segment $[i-1, i]$ are the elements of the so-called parameter vector (see [13])

$$\boldsymbol{m} = (m_1, m_2, m_3)^T = \sqrt{\rho}(1, u, H)^T. \tag{23}$$

Therefore, its average value on $[i-1, i]$ is

$$\tilde{\boldsymbol{m}} = \frac{\boldsymbol{m}_{i-1} + \boldsymbol{m}_i}{2} \tag{24}$$

Thus the following Roe-averaged quantities can be defined

$$\begin{aligned} \rho^* &= \tilde{m}_1^2 \\ \tilde{u} &= \tilde{m}_2/\tilde{m}_1 \\ \tilde{H} &= \tilde{m}_3/\tilde{m}_1 \end{aligned} \tag{25}$$

and

$$\tilde{c}^2 = (\gamma - 1)(\tilde{H} - \frac{\tilde{u}^2}{2}) \tag{26}$$

Introducing the Roe-averaged Jacobian $\tilde{A} \equiv \tilde{A}(u_{i-1}, u_i)$ and recalling (21) we can rewrite the fluctuation (22) in the following form

$$\boldsymbol{R} = -\tilde{A} \cdot (\boldsymbol{u}_i - \boldsymbol{u}_{i-1}). \tag{27}$$

Having in mind the construction of an upwind scheme, it is convenient to use the following representation of the matrix $\tilde{A}$ (see [13])

$$\tilde{A} = \tilde{T}\tilde{\Lambda}\tilde{T}^{-1}, \tag{28}$$

where $\tilde{\Lambda}$ is a diagonal matrix

$$\tilde{\Lambda} = \begin{pmatrix} \lambda_1 & 0 & 0 \\ 0 & \lambda_2 & 0 \\ 0 & 0 & \lambda_3 \end{pmatrix}, \tag{29}$$

where

$$\lambda_1 = \tilde{u}, \quad \lambda_{2,3} = \tilde{u} \pm \tilde{c}$$

are the eigenvalues and $\tilde{T} = (\tilde{\boldsymbol{E}}^1, \tilde{\boldsymbol{E}}^2, \tilde{\boldsymbol{E}}^3)$ is the matrix of right eigenvectors of $\tilde{A}$

$$\tilde{\boldsymbol{E}}^1 = \begin{pmatrix} 1 \\ \tilde{u} \\ \tilde{u}^2/2 \end{pmatrix}; \quad \tilde{\boldsymbol{E}}^2 = \begin{pmatrix} 1 \\ \tilde{u} - \tilde{c} \\ \tilde{H} - \tilde{u}\tilde{c} \end{pmatrix}; \quad \tilde{\boldsymbol{E}}^3 = \begin{pmatrix} 1 \\ \tilde{u} + \tilde{c} \\ \tilde{H} + \tilde{u}\tilde{c} \end{pmatrix}. \tag{30}$$

The fluctuation-splitting formulation of the Roe scheme can be written as follows

$$\begin{aligned} h\boldsymbol{u}_{i-1}^{n+1} &= h\boldsymbol{u}_{i-1}^{n} + \tfrac{\tau}{2}(\boldsymbol{R} + \bar{\boldsymbol{R}}) \\ h\boldsymbol{u}_{i}^{n+1} &= h\boldsymbol{u}_{i}^{n} + \tfrac{\tau}{2}(\boldsymbol{R} - \bar{\boldsymbol{R}}), \end{aligned} \tag{31}$$

where

$$\bar{\boldsymbol{R}} = -\tilde{T}|\tilde{\Lambda}|(\boldsymbol{w}_i - \boldsymbol{w}_{i-1}) \tag{32}$$

is the artificial viscosity, and

$$\boldsymbol{w} = \tilde{T}^{-1}\boldsymbol{u} \tag{33}$$

are the so-called characteristic variables.

Alternatively, the artificial viscosity can be also written as

$$\bar{\boldsymbol{R}} = -|\tilde{A}|(\boldsymbol{u}_i - \boldsymbol{u}_{i-1}) \tag{34}$$

or

$$\bar{\boldsymbol{R}} = -\mathrm{sign}(\tilde{A})\boldsymbol{R} \tag{35}$$

3.2. Roe scheme revisited. It is convenient for the purpose of this work to introduce the following *auxiliary* variables $(s, u, p)^T$, where

$$ds = d\rho - \frac{dp}{c^2} \tag{36}$$

is the entropy. The non-conservative formulation of the Euler equations in these variables takes the following form

$$\begin{aligned} &s_t + u s_x = 0 \\ &\rho u_t + \rho u u_x + p_x = 0 \\ &p_t + u p_x + \rho c^2 u_x = 0 \end{aligned} \tag{37}$$

Introduce the fluctuations of the Euler equations in the auxiliary variables

$$\boldsymbol{r} = -\tilde{A} \cdot \begin{pmatrix} s_i - s_{i-1} \\ \rho^*(u_i - u_{i-1}) \\ p_i - p_{i-1} \end{pmatrix}, \tag{38}$$

where

$$\tilde{A} = \begin{pmatrix} \tilde{u} & 0 & 0 \\ 0 & \tilde{u} & 1 \\ 0 & \tilde{c}^2 & \tilde{u} \end{pmatrix} \tag{39}$$

It can be easily verified that

$$\boldsymbol{R} = C_a \boldsymbol{r}, \tag{40}$$

where

$$C_a = \begin{pmatrix} 1 & 0 & 1/\tilde{c}^2 \\ \tilde{u} & 1 & \tilde{u}/\tilde{c}^2 \\ \tilde{u}^2/2 & \tilde{u} & 1/(\gamma-1) + u^2/(2c^2) \end{pmatrix} \tag{41}$$

Therefore, the Roe scheme (31) can be written as follows

$$\begin{aligned} h\boldsymbol{u}_{i-1}^{n+1} &= h\boldsymbol{u}_{i-1}^{n} + \tfrac{\tau}{2} C_a(\boldsymbol{r} + \bar{\boldsymbol{r}}) \\ h\boldsymbol{u}_{i}^{n+1} &= h\boldsymbol{u}_{i}^{n} + \tfrac{\tau}{2} C_a(\boldsymbol{r} - \bar{\boldsymbol{r}}) \end{aligned} \tag{42}$$

where the artificial viscosity

$$\bar{\boldsymbol{r}} = C_a^{-1} \bar{\boldsymbol{R}} = -C_a^{-1} \tilde{T} |\tilde{\Lambda}| [\boldsymbol{w}_i - \boldsymbol{w}_{i-1}] \tag{43}$$

with

$$C_a^{-1} = \begin{pmatrix} 1 - (\gamma-1)\tilde{u}/(2\tilde{c}^2) & (\gamma-1)\tilde{u}/\tilde{c}^2 & -(\gamma-1)/\tilde{c}^2 \\ -\tilde{u} & 1 & 0 \\ (\gamma-1)\tilde{u}^2/(2\tilde{c}^2) & -(\gamma-1)\tilde{u} & \gamma-1 \end{pmatrix} \tag{44}$$

We can also write

$$\bar{\boldsymbol{r}} = -|\tilde{A}| \cdot \begin{pmatrix} s_i - s_{i-1} \\ \rho^*(u_i - u_{i-1}) \\ p_i - p_{i-1} \end{pmatrix} \tag{45}$$

or

$$\bar{\boldsymbol{r}} = \operatorname{sign}(\tilde{A})\boldsymbol{r} \tag{46}$$

It is evident from (43) and (45) that the matrix of right eigenvectors of $\tilde{A}$ is

$$\tilde{T} = C_a^{-1}\tilde{T}$$

or $\tilde{T} = (\tilde{\boldsymbol{e}}_1, \tilde{\boldsymbol{e}}_2, \tilde{\boldsymbol{e}}_3)$ where

$$\tilde{\boldsymbol{e}}_1 = \begin{pmatrix} 1 \\ 0 \\ 0 \end{pmatrix}; \quad \tilde{\boldsymbol{e}}_2 = \begin{pmatrix} 0 \\ -\tilde{c} \\ \tilde{c}^2 \end{pmatrix}; \quad \tilde{\boldsymbol{e}}_3 = \begin{pmatrix} 0 \\ \tilde{c} \\ \tilde{c}^2 \end{pmatrix} \tag{47}$$

REMARK 3.1. *It is obvious from the structure of the matrix $\tilde{T}$ that the auxiliary variable s coincides with the first element of the characteristic variable vector (33)*

$$w_1 = s \tag{48}$$

Denote

$$M = \operatorname{sign}(\tilde{A})$$

In order to make a computer program more efficient it is useful to write an explicit expression for the matrix M. It is easy to see that in the supersonic case

$$M^{sup} = \operatorname{sign}(\tilde{u}) \cdot I \tag{49}$$

where I is a 3×3 unity matrix.

Some algebra reveals that in the subsonic case matrix $\operatorname{sign}(\tilde{A})$ has a very simple structure as well

$$M^{sub} = \begin{pmatrix} \operatorname{sign}(\tilde{u}) & 0 & 0 \\ 0 & 0 & 1/\tilde{c} \\ 0 & \tilde{c} & 0 \end{pmatrix} \tag{50}$$

The second and third rows mean that the artificial diffusion added to the momentum equations is proportional to the fluctuation of the pressure equation and vice versa.

REMARK 3.2. *The* auxiliary *variables formulation (37) of the Euler equations is, perhaps, the simplest way to write the Euler equations. The usefulness of this formulation will become even more evident in §§4,6.*

4. Construction of the two-dimensional Euler scheme. The Euler equations of gas dynamics in two dimensions can be written

$$\boldsymbol{u}_t + \boldsymbol{F}(\boldsymbol{u})_x + \boldsymbol{G}(\boldsymbol{u})_y = \mathbf{o}, \tag{51}$$

where

$$\boldsymbol{u} = \begin{pmatrix} \rho \\ \rho u \\ \rho v \\ e \end{pmatrix}; \quad \boldsymbol{F}(\boldsymbol{u}) = \begin{pmatrix} \rho u \\ \rho u^2 + p \\ \rho uv \\ \rho uH \end{pmatrix}; \quad \boldsymbol{G}(\boldsymbol{u}) = \begin{pmatrix} \rho v \\ \rho uv \\ \rho v^2 + p \\ \rho vH \end{pmatrix} \tag{52}$$

where the enthalpy H is defined by

$$H = \frac{e+p}{\rho} = \frac{c^2}{\gamma-1} + \frac{u^2+v^2}{2}, \tag{53}$$

the speed of sound

$$c = \sqrt{\frac{\gamma p}{\rho}} \tag{54}$$

and the pressure

$$p = (\gamma-1)(e - \rho\frac{u^2+v^2}{2}) \tag{55}$$

The quasilinear non-conservative formulation of the Euler system in *auxiliary* variables (s,u,v,p) can be introduced in two dimensions as well

$$\begin{aligned} &s_t + us_x + vs_y = 0 \\ &\rho u_t + \rho u u_x + \rho v u_y + p_x = 0 \\ &\rho v_t + \rho u v_x + \rho v v_y + p_y = 0 \\ &p_t + up_x + vp_y + \rho c^2(u_x + v_y) = 0 \end{aligned} \tag{56}$$

where $ds = d\rho - \frac{dp}{c^2}$.

REMARK 4.1. *Note that the entropy (s) evolution is subject to the two-dimensional advection equation, which is locally decoupled from the rest of the system.*

The fluctuation of the system (51) defined over the triangle T

$$\boldsymbol{R} = \int\int \boldsymbol{u}_t = -\int\int (\boldsymbol{F}_x + \boldsymbol{G}_y)\, dx\, dy = -S_T \left[\widehat{\boldsymbol{F}}_x + \widehat{\boldsymbol{G}}_y\right] \tag{57}$$

where $\widehat{\boldsymbol{F}}_x, \widehat{\boldsymbol{G}}_y$ are some averaged values of the flux derivatives over the triangle T.

Our construction of the truly two-dimensional Euler scheme utilizes the two dimensional extension (Roe, Struijs and Deconinck [16]) of the Roe conservative linearization for one-dimensional case. Therefore, following the procedure developed in [16], we assume that the quantity which varies linearly over an element is the "parameter vector"

$$\boldsymbol{m} = \sqrt{\rho}(1, u, v, H)^T \tag{58}$$

and its averaged value on the triangle T (as illustrated on Fig.2) is given by the following

$$\tilde{\boldsymbol{m}} = \frac{\boldsymbol{m}_0 + \boldsymbol{m}_3 + \boldsymbol{m}_4}{3} \tag{59}$$

Roe-averaged quantities can be introduced

$$\begin{aligned} \tilde{u} &= \tilde{m}_2/\tilde{m}_1 \\ \tilde{v} &= \tilde{m}_3/\tilde{m}_1 \\ \tilde{H} &= \tilde{m}_4/\tilde{m}_1 \end{aligned} \tag{60}$$

and

$$\tilde{c}^2 = (\gamma-1)[\tilde{H} - \frac{1}{2}(\tilde{u}^2 + \tilde{v}^2)] \tag{61}$$

Fluctuations of the Euler system in the *auxiliary* variables can be presented as

$$\boldsymbol{r} = \boldsymbol{r}^x + \boldsymbol{r}^y, \tag{62}$$

where

$$\begin{aligned} \boldsymbol{r}^x &= -S_T \tilde{A} \cdot (\widehat{s_x}, \widehat{\rho u_x}, \widehat{\rho v_x}, \widehat{p_x})^T \\ \boldsymbol{r}^y &= -S_T \tilde{B} \cdot (\widehat{s_y}, \widehat{\rho u_y}, \widehat{\rho v_y}, \widehat{p_y})^T \end{aligned}$$

with

$$\tilde{A} = \begin{pmatrix} \tilde{u} & 0 & 0 & 0 \\ 0 & \tilde{u} & 0 & 1 \\ 0 & 0 & \tilde{u} & 0 \\ 0 & \tilde{c}^2 & 0 & \tilde{u} \end{pmatrix}, \quad \tilde{B} = \begin{pmatrix} \tilde{v} & 0 & 0 & 0 \\ 0 & \tilde{v} & 0 & 0 \\ 0 & 0 & \tilde{v} & 1 \\ 0 & 0 & \tilde{c}^2 & \tilde{v} \end{pmatrix}$$

and $S_T = h^2/2$ is the area of the triangle T, and

$$\widehat{\rho_x} = 2\tilde{m}_1 (m_1)_x \tag{63}$$

$$\widehat{\rho u_x} = \tilde{m}_1 (m_2)_x - \tilde{m}_2 (m_1)_x \tag{64}$$

$$\widehat{\rho v_x} = \tilde{m}_1 (m_3)_x - \tilde{m}_3 (m_1)_x \tag{65}$$

$$\widehat{p_x} = \frac{\gamma - 1}{\gamma} [(\tilde{m}_4 (m_1)_x + \tilde{m}_1 (m_4)_x) + (\tilde{m}_2 (m_2)_x + \tilde{m}_3 (m_3)_x)] \tag{66}$$

The corresponding terms involving derivatives in the y direction can be written in the analogous manner.

Introducing the matrix

$$C_a = \begin{pmatrix} 1 & 0 & 0 & 1/\tilde{c}^2 \\ \tilde{u} & 1 & 0 & \tilde{u}/\tilde{c}^2 \\ \tilde{v} & 0 & 1 & \tilde{v}/\tilde{c}^2 \\ (\tilde{u}^2 + \tilde{v}^2)/2 & \tilde{u} & \tilde{v} & 1/(\gamma - 1) + (\tilde{u}^2 + \tilde{v}^2)/(2\tilde{c}^2) \end{pmatrix} \tag{67}$$

we can define

$$\begin{aligned} \boldsymbol{R}^x &= C_a \boldsymbol{r}^x \\ \boldsymbol{R}^y &= C_a \boldsymbol{r}^y \end{aligned} \tag{68}$$

It can be easily verified that

$$\begin{aligned} \boldsymbol{R}^x &= -S^T \widehat{\boldsymbol{F}_x} \\ \boldsymbol{R}^y &= -S^T \widehat{\boldsymbol{G}_y}, \end{aligned} \tag{69}$$

where $\widehat{\boldsymbol{F}_x}, \widehat{\boldsymbol{G}_y}$ are the same averaged flux derivative values as defined in [16]. It is also obvious that the entire fluctuation

$$\boldsymbol{R} = \boldsymbol{R}^x + \boldsymbol{R}^y = C_a (\boldsymbol{r}^x + \boldsymbol{r}^y) = C_a \boldsymbol{r} \tag{70}$$

Consider triangle T as illustrated in Fig.2. The fluctuation is distributed according to the following formulae:

$$\begin{aligned} S\boldsymbol{u}_0^{n+1} &= S\boldsymbol{u}_0^n + \tfrac{\tau}{2} C_a (\boldsymbol{r}^x - \bar{\boldsymbol{r}}^x) \\ S\boldsymbol{u}_3^{n+1} &= S\boldsymbol{u}_3^n + \tfrac{\tau}{2} C_a [(\boldsymbol{r}^x + \bar{\boldsymbol{r}}^x) + (\boldsymbol{r}^y - \bar{\boldsymbol{r}}^y)] \\ S\boldsymbol{u}_4^{n+1} &= S\boldsymbol{u}_4^n + \tfrac{\tau}{2} C_a (\boldsymbol{r}^y + \bar{\boldsymbol{r}}^y) \end{aligned} \tag{71}$$

Defining

$$\bar{\boldsymbol{r}}^x = \mathrm{sign}(\tilde{A})\boldsymbol{r}^x \qquad (72)$$
$$\bar{\boldsymbol{r}}^y = \mathrm{sign}(\tilde{B})\boldsymbol{r}^y$$

we obtain the scheme that is similar to the standard Roe dimensionally split scheme. The only difference is in the linearization procedure.

We can construct now a (linearity preserving) second order accurate scheme. First, we shall introduce vectors $\boldsymbol{r}^{x^*}, \boldsymbol{r}^{y^*}$ with their elements defined by

$$r_i^{x^*} = r_i^x + \Psi(q_i) r_i^y \qquad (73)$$
$$r_i^{y^*} = r_i^y + \frac{\Psi(q_i)}{q_i} r_i^x$$

for $i = 1, 2, 3, 4$, where

$$q_i = -\frac{r_i^x}{r_i^y} \qquad (74)$$

and Ψ is a (non-compressive) limiter.

Substituting $\boldsymbol{r}^{x^*}, \boldsymbol{r}^{y^*}$ for $\boldsymbol{r}^x, \boldsymbol{r}^y$ in (71) and (72) we obtain a genuinely two-dimensional scheme, which is also linearity preserving (second order accurate in this case). This is because if

$$\boldsymbol{r} = 0$$

then

$$\boldsymbol{r}^{x^*} = \boldsymbol{r}^{y^*} = 0$$

as well. Therefore, the update of any variable in all the three vertices of the triangle T due to the fluctuation on this triangle is zero.

The resulting scheme is also conservative since

$$\boldsymbol{r} \equiv \boldsymbol{r}^x + \boldsymbol{r}^y \equiv \boldsymbol{r}^{x^*} + \boldsymbol{r}^{y^*}$$

Some attributes and properties of the genuinely multidimensional schemes will be discussed later in §9.3. It is important for the purpose of this discussion to write down the explicit expressions for the matrices $\mathrm{sign}(\tilde{A}), \mathrm{sign}(\tilde{B})$. Denote

$$M_x = \mathrm{sign}(\tilde{A})$$
$$M_y = \mathrm{sign}(\tilde{B})$$

For matrix M_x the distinction should be made between two cases

$$M_x = \begin{cases} M_x^{sub}, & \text{if } |\tilde{u}| \le \tilde{c} \\ M_x^{sup}, & \text{if } |\tilde{u}| > \tilde{c}, \end{cases} \qquad (75)$$

and similarly

$$M_y = \begin{cases} M_y^{sub}, & \text{if } |\tilde{v}| \le \tilde{c} \\ M_y^{sup}, & \text{if } |\tilde{v}| > \tilde{c}, \end{cases} \qquad (76)$$

where

$$M_x^{sup} = \text{sign}(\tilde{u})I, \tag{77}$$

$$M_y^{sup} = \text{sign}(\tilde{v})I. \tag{78}$$

and I is the 4×4 unity matrix. These matrices for the subsonic case appear to be very simple as well

$$M_x^{sub} = \begin{pmatrix} \text{sign}(\tilde{u}) & 0 & 0 & 0 \\ 0 & 0 & 0 & 1/\tilde{c} \\ 0 & 0 & \text{sign}(\tilde{u}) & 0 \\ 0 & \tilde{c} & 0 & 0 \end{pmatrix}, \tag{79}$$

$$M_y^{sub} = \begin{pmatrix} \text{sign}(\tilde{v}) & 0 & 0 & 0 \\ 0 & \text{sign}(\tilde{v}) & 0 & 0 \\ 0 & 0 & 0 & 1/\tilde{c} \\ 0 & 0 & \tilde{c} & 0 \end{pmatrix} \tag{80}$$

and their structure may have a very important meaning (see §9.3).

5. General unstructured grid formulation. Consider an unstructured triangular grid covering our domain and triangle T belonging to this grid (see Fig.4). Denote by h_i the length of the ith face of this triangle, $\vec{e}_i$ a unit vector along the ith face in the clockwise direction. Denote also $\vec{n}_i$ a unit inward normal to the ith face and S_T - area of the triangle T. In this section we shall describe first the general (unstructured grid) version of the fluctuation-splitting advection scheme. Then we shall construct the genuinely two-dimensional numerical scheme for the compressible Euler system, also formulated for unstructured meshes.

5.1. Advection scheme. Consider a linear constant coefficient advection equation

$$u_t + \vec{\lambda} \cdot \vec{\nabla} u = 0 \tag{81}$$

Consider a non-orthogonal coordinate system ξ, η aligned with the vectors e_1, e_2 (see Fig.4) and introduce the following quantities

$$\alpha = \frac{\vec{\lambda} \cdot \vec{n}_2}{\theta}, \quad \beta = \frac{\vec{\lambda} \cdot \vec{n}_1}{\theta} \tag{82}$$

where

$$\theta = \vec{e}_1 \cdot \vec{n}_2 \equiv \vec{e}_2 \cdot \vec{n}_1. \tag{83}$$

Then Eq.(81) can be written in the coordinate system ξ, η

$$u_t + \alpha u_\xi + \beta u_\eta = 0 \tag{84}$$

The fluctuation of the Eq.(81)

$$R = R^\xi + R^\eta, \tag{85}$$

where

$$R^{\xi} = -S_T[\alpha(u_3 - u_1)/h_1] \qquad (86)$$
$$R^{\eta} = -S_T[\beta(u_2 - u_3)/h_2]$$

The fluctuation distribution formulae

$$S_1 u_1^{n+1} = S_1 u_1^n + \tfrac{\tau}{2}(R^{\xi} - \bar{R}^{\xi}) \qquad (87)$$
$$S_2 u_2^{n+1} = S_2 u_2^n + \tfrac{\tau}{2}(R^{\eta} + \bar{R}^{\eta})$$
$$S_3 u_3^{n+1} = S_3 u_3^n + \tfrac{\tau}{2}[(R^{\xi} + \bar{R}^{\xi}) + (R^{\eta} - \bar{R}^{\eta})]$$

with the artificial viscosity terms defined as follows

$$\bar{R}^{\xi} = \mathrm{sign}(\alpha) R^{\xi} \qquad (88)$$
$$\bar{R}^{\eta} = \mathrm{sign}(\beta) R^{\eta}$$

result in a positive type upwind scheme. Introduce the following quantity

$$Q = -\frac{R^{\xi}}{R^{\eta}} \qquad (89)$$

Define

$$R^{\xi^*} = R^{\xi} + R^{\eta}\Psi(Q) \qquad (90)$$
$$R^{\eta^*} = R^{\eta} + R^{\xi}\frac{\Psi(Q)}{Q}$$

and substitute R^{ξ^*}, R^{η^*} instead of R^{ξ}, R^{η} in (87),(88). Using the identity

$$R^{\eta}\Psi(Q) \equiv -R^{\xi}\frac{\Psi(Q)}{Q} \qquad (91)$$

we can rewrite R^{ξ^*}, R^{η^*} in the following form

$$R^{\xi^*} = R^{\xi}(1 - \tfrac{\Psi(Q)}{Q}) \qquad (92)$$
$$R^{\eta^*} = R^{\eta}(1 - \Psi(Q)).$$

It is easy to verify that the resulting scheme is positive if

$$0 \le \Psi(Q) \le 1, \quad 0 \le \frac{\Psi(Q)}{Q} \le 1 \qquad (93)$$

and linearity preserving if

$$\Psi(1) = 1 \qquad (94)$$

Note also that

$$R = R^{\xi^*} + R^{\eta^*} = R^{\xi} + R^{\eta}. \qquad (95)$$

Therefore, the constructed scheme is conservative.

There are two differences between the formulated scheme and the typical fluctuation splitting advection schemes (see [6],[22],[19])

1. no distinction is made between triangles with two outflow faces (Type I) and one outflow face (Type II)
   For the advection problem this implies more computational work since the limiter function has to be evaluated on all the triangles (not only on those of Type II). However, for the Euler system no significant savings can be made by this distinction, since limiters have to be used on all the triangles anyway (see §5.2).
2. the derivatives are approximated by finite differences along the faces which were chosen arbitrarily and are not necessarily both inflow or outflow (α and β are not necessarily of the same sign).
   In the case of advection, the choice of faces which are both either inflow or outflow for derivative approximation provides better resolution of discontinuities. For systems, however, the question of the optimal choice is more complex (see remark in §8). Therefore, we presented here the construction of the advection scheme with no assumption made about the signs of α and β.

5.2. Euler system. The *auxiliary* variable formulation of the Euler system can be written in the following vector form

$$
\begin{aligned}
& s_t + \vec{U} \cdot \nabla s = 0 \\
& \rho \vec{U}_t + \rho \vec{U} \cdot \nabla \vec{U} + \nabla p = 0 \\
& p_t + \vec{U} \cdot \nabla p + \rho c^2 \nabla \cdot \vec{U} = 0
\end{aligned} \tag{96}
$$

where $\vec{U} = (u, v)$

Consider again triangle T on Fig.4 and the non-orthogonal coordinate system (ξ, η) aligning with two of the faces of this triangle (or the unit vectors $\vec{e}_1, \vec{e}_2$) Define the following quantities

$$
\mathcal{U} = \vec{U} \cdot \vec{e}_2, \quad \mathcal{V} = \vec{U} \cdot \vec{e}_1. \tag{97}
$$

and

$$
\alpha = \frac{\vec{U} \cdot \vec{n}_1}{\theta}, \quad \beta = \frac{\vec{U} \cdot \vec{n}_2}{\theta}. \tag{98}
$$

We can rewrite the Euler system (96) in this new non-orthogonal coordinates (ξ, η)

$$
\begin{aligned}
& s_t + \alpha s_\xi + \beta s_\eta = 0 \\
& \rho \mathcal{U}_t + \rho \alpha \mathcal{U}_\xi + \rho \beta \mathcal{U}_\eta + p_\xi = 0 \\
& \rho \mathcal{V}_t + \rho \alpha \mathcal{V}_\xi + \rho \beta \mathcal{V}_\eta + p_\eta = 0 \\
& p_t + \alpha p_\xi + \beta p_\eta + \rho c^2 (\alpha_\xi + \beta_\eta) = 0
\end{aligned} \tag{99}
$$

In order to compute the fluctuation of the system

$$
\boldsymbol{r} = \boldsymbol{r}^\xi + \boldsymbol{r}^\eta \tag{100}
$$

on a general triangle T we follow again the two-dimensional linearization procedure presented in [16] and assume the quantity varying linearly on the triangle is the parameter vector

$$
\boldsymbol{m} = \sqrt{\rho}(1, u, v, H)^T \tag{101}
$$

and its averaged value on the triangle T is given by the following

$$\tilde{\boldsymbol{m}} = \frac{\boldsymbol{m}_1 + \boldsymbol{m}_2 + \boldsymbol{m}_3}{3} \tag{102}$$

Then (similarly to the structured grid case)

$$\boldsymbol{r}^{\xi} = -S_T \begin{pmatrix} \tilde{\alpha}\hat{s_\xi} \\ \tilde{\alpha}\widehat{\rho\mathcal{U}_\xi} + \widehat{p_\xi} \\ \tilde{\alpha}\widehat{\rho\mathcal{V}_\xi} \\ \tilde{\alpha}\widehat{p_\xi} + \tilde{c}^2\widehat{\rho\alpha_\xi} \end{pmatrix} \tag{103}$$

where

$$\widehat{\rho_\xi} = 2\tilde{m}_1(m_1)_\xi \tag{104}$$

$$\widehat{p_\xi} = \frac{\gamma - 1}{\gamma}[(\tilde{m}_4(m_1)_\xi + \tilde{m}_1(m_4)_\xi) + (\tilde{m}_2(m_2)_\xi + \tilde{m}_3(m_3)_\xi)] \tag{105}$$

$$\hat{s}_\xi = \widehat{p_\xi} - \tilde{c}^2\widehat{\rho_\xi} \tag{106}$$

$$\widehat{\rho\vec{U}_\xi} = \begin{pmatrix} \widehat{\rho u_\xi} \\ \widehat{\rho v_\xi} \end{pmatrix} = \begin{pmatrix} \tilde{m}_1(m_2)_\xi - \tilde{m}_2(m_1)_\xi \\ \tilde{m}_1(m_3)_\xi - \tilde{m}_3(m_1)_\xi \end{pmatrix} \tag{107}$$

$\boldsymbol{r}^{\eta}$ can be evaluated in a similar way. Defining the following set of conservative variables

$$\breve{\boldsymbol{u}} = \begin{pmatrix} \rho \\ \rho\mathcal{U} \\ \rho\mathcal{V} \\ e \end{pmatrix} \tag{108}$$

and denoting $\breve{\boldsymbol{R}}$ the fluctuations of the Euler system in these variables on triangle T, it can be easily verified that the fluctuations in the following relation holds

$$\breve{\boldsymbol{R}} = C_a \cdot \boldsymbol{r} \tag{109}$$

where

$$C_a = \begin{pmatrix} 1 & 0 & 0 & 1/\tilde{c}^2 \\ \tilde{\mathcal{U}} & 1 & 0 & \tilde{\mathcal{U}}/\tilde{c}^2 \\ \tilde{\mathcal{V}} & 0 & 1 & \tilde{\mathcal{V}}/\tilde{c}^2 \\ \tilde{U}^2/2 & \tilde{\alpha} & \tilde{\beta} & 1/(\gamma-1) + \tilde{U}^2/(2\tilde{c}^2) \end{pmatrix} \tag{110}$$

The fluctuation distribution formulae

$$\begin{aligned} S_1\breve{\boldsymbol{u}}_1^{n+1} &= S_1\breve{\boldsymbol{u}}_1^{n} + \tfrac{\tau}{2}C_a(\boldsymbol{r}^{\xi} - \bar{\boldsymbol{r}}^{\xi}) \\ S_2\breve{\boldsymbol{u}}_2^{n+1} &= S_2\breve{\boldsymbol{u}}_2^{n} + \tfrac{\tau}{2}C_a(\boldsymbol{r}^{\eta} + \bar{\boldsymbol{r}}^{\eta}) \\ S_3\breve{\boldsymbol{u}}_3^{n+1} &= S_3\breve{\boldsymbol{u}}_3^{n} + \tfrac{\tau}{2}C_a[(\boldsymbol{r}^{\xi} + \bar{\boldsymbol{r}}^{\xi}) + (\boldsymbol{r}^{\eta} - \bar{\boldsymbol{r}}^{\eta})] \end{aligned} \tag{111}$$

will result in an upwind scheme provided we define the artificial viscosity terms $\bar{\boldsymbol{r}}^{\xi}, \bar{\boldsymbol{r}}^{\eta}$. However, before doing this we would like to rewrite (111) for the update of the "regular" conservative variables $\boldsymbol{u} = (\rho, \rho u, \rho v, e)^T$. Note that

$$\boldsymbol{u} = \Theta \cdot \breve{\boldsymbol{u}} \tag{112}$$

where

$$\Theta = \begin{pmatrix} 1 & 0 & 0 & 0 \\ 0 & n_1^x/\theta & n_1^y/\theta & 0 \\ 0 & n_2^x/\theta & n_2^y/\theta & 0 \\ 0 & 0 & 0 & 1 \end{pmatrix} \tag{113}$$

Introducing the following matrix

$$\tilde{C}_a^\theta = \Theta \cdot C_a = \begin{pmatrix} 1 & 0 & 0 & 1/\tilde{c}^2 \\ \tilde{u} & n_1^x/\theta & n_1^y/\theta & \tilde{u}/\tilde{c}^2 \\ \tilde{v} & n_2^x/\theta & n_2^y/\theta & \tilde{v}/\tilde{c}^2 \\ \tilde{U}^2/2 & \tilde{\alpha} & \tilde{\beta} & 1/(\gamma-1) + \tilde{U}^2/(2\tilde{c}^2) \end{pmatrix} \tag{114}$$

we obtain the fluctuation distribution formulae for the "regular" conservative variables

$$\begin{array}{lll} S_1 \boldsymbol{u}_1^{n+1} & = S_1 \boldsymbol{u}_1^n & + \frac{\tau}{2} C_a^\theta (\boldsymbol{r}^\xi - \bar{\boldsymbol{r}}^\xi) \\ S_2 \boldsymbol{u}_2^{n+1} & = S_2 \boldsymbol{u}_2^n & + \frac{\tau}{2} C_a^\theta (\boldsymbol{r}^\eta + \bar{\boldsymbol{r}}^\eta) \\ S_3 \boldsymbol{u}_3^{n+1} & = S_3 \boldsymbol{u}_3^n & + \frac{\tau}{2} C_a^\theta [(\boldsymbol{r}^\xi + \bar{\boldsymbol{r}}^\xi) + (\boldsymbol{r}^\eta - \bar{\boldsymbol{r}}^\eta)] \end{array} \tag{115}$$

The relationship between the artificial viscosity and the fluctuations is given by

$$\begin{aligned} \bar{\boldsymbol{r}}^\xi &= M_\xi \boldsymbol{r}^\xi \\ \bar{\boldsymbol{r}}^\eta &= M_\eta \boldsymbol{r}^\eta \end{aligned} \tag{116}$$

where

$$M_\xi = \begin{cases} M_\xi^{sub}, & \text{if } |\tilde{\alpha}| \le \tilde{c} \\ M_\xi^{sup}, & \text{if } |\tilde{\alpha}| > \tilde{c}, \end{cases} \tag{117}$$

and

$$M_\eta = \begin{cases} M_\eta^{sub}, & \text{if } |\tilde{\beta}| \le \tilde{c} \\ M_\eta^{sup}, & \text{if } |\tilde{\beta}| > \tilde{c}, \end{cases} \tag{118}$$

$$M_\xi^{sub} = \begin{pmatrix} \text{sign}(\tilde{\alpha}) & 0 & 0 & 0 \\ 0 & 0 & 0 & 1/\tilde{c} \\ 0 & 0 & \text{sign}(\tilde{\alpha}) & 0 \\ 0 & \tilde{c} & 0 & 0 \end{pmatrix}, \tag{119}$$

$$M_\eta^{sub} = \begin{pmatrix} \text{sign}(\tilde{\beta}) & 0 & 0 & 0 \\ 0 & \text{sign}(\tilde{\beta}) & 0 & 0 \\ 0 & 0 & 0 & 1/\tilde{c} \\ 0 & 0 & \tilde{c} & 0 \end{pmatrix}, \tag{120}$$

and

$$M_\xi^{sup} = \text{sign}(\tilde{\alpha}) I, \tag{121}$$

$$M_\eta^{sup} = \text{sign}(\tilde{\beta}) I. \tag{122}$$

A linearity preserving genuinely two-dimensional scheme can be constructed by introducing the vectors r^{ξ^*}, r^{η^*} with their elements defined by

$$
\begin{aligned}
r_i^{\xi^*} &= r_i^{\xi} + \Psi(q_i) r_i^{\eta} \\
r_i^{\eta^*} &= r_i^{\eta} + \frac{\Psi(q_i)}{q_i} r_i^{\xi}
\end{aligned}
\tag{123}
$$

for $i = 1, 2, 3, 4$, where

$$
q_i = -\frac{r_i^{\xi}}{r_i^{\eta}}
\tag{124}
$$

and substituting them instead of r^{ξ}, r^{η} respectively in (115),(116).

REMARK 5.1. *In order to construct a non-oscillatory linearity preserving scheme for the Euler equations, derivatives can be approximated along any two out of three faces of the triangle. However, the resolution of such features of the flow as shocks, contact discontinuities and shear layers can be affected by the particular choice (see §8). Shocks are being resolved better (i.e. are represented by sharper numerical layers) if the numerical derivatives are computed along those two faces of the triangle which are the closest to the direction of the shock. The same is true for the shear layers and contact discontinuities, although the two faces closest to the discontinuity direction in this case will also be either two inflow or outflow faces of the triangle.*

6. Outline of the extension to three dimensions. A detailed description of the three-dimensional schemes both for the scalar advection and Euler system will be given elsewhere. In this paper we only outline briefly their construction in the case of structured Cartesian grids. Each cube having grid nodes as its vertices can be divided into two prisms. The prisms can be divided into three tetrahedra each. Any of the obtained tetrahedra will have 3 of its edges parallel to the x, y and z axes respectively. We shall utilize this in this section to make the presentation free of unnecessary details related to the non-orthogonal coordinate systems. The construction of the fluctuation-splitting schemes both for the scalar advection and the Euler system will be outlined for the case of the tetrahedron T as illustrated on Fig.5.

6.1. Advection scheme in three dimensions. Consider a scalar constant coefficient advection equation in three dimensions

$$
u_t + a u_x + b u_y + c u_z = 0
\tag{125}
$$

The fluctuation of this equation on the tetrahedron T (see Fig.5), whose volume is $V = h^3/6$.

$$
R = R^x + R^y + R^z
\tag{126}
$$

where

$$
\begin{aligned}
R^x &= -\tfrac{h^2}{6}[a(u_3 - u_4)] \\
R^y &= -\tfrac{h^2}{6}[b(u_2 - u_3)] \\
R^z &= -\tfrac{h^2}{6}[c(u_1 - u_2)]
\end{aligned}
\tag{127}
$$

The fluctuation distribution formulae are given as follows

$$
\begin{aligned}
V u_1^{n+1} &= V u_1^n + \tfrac{\tau}{2} C_a (R^z + \bar{R}^z) \\
V u_2^{n+1} &= V u_2^n + \tfrac{\tau}{2} C_a [(R^y + \bar{R}^y) + (R^z - \bar{R}^z)] \\
V u_3^{n+1} &= V u_3^n + \tfrac{\tau}{2} C_a [(R^x + \bar{R}^x) + (R^y - \bar{R}^y)] \\
V u_4^{n+1} &= V u_4^n + \tfrac{\tau}{2} C_a (R^x - \bar{R}^x)
\end{aligned}
\tag{128}
$$

It is easy to see that the following choice of the artificial viscosity

$$\begin{aligned} \bar{R}^x &= \text{sign}(a)R^x \\ \bar{R}^y &= \text{sign}(b)R^y \\ \bar{R}^z &= \text{sign}(c)R^z \end{aligned} \tag{129}$$

results in a regular upwind scheme.

Introducing the following quantities

$$Q^x = \frac{[R^y]_x^- + [R^z]_x^-}{R^x + [R^y]_x^+ + [R^z]_x^+} \tag{130a}$$

$$Q^y = \frac{[R^x]_y^- + [R^z]_y^-}{R_y + [R^x]_y^+ + [R^z]_y^+} \tag{130b}$$

$$Q^z = \frac{[R^x]_z^- + [R^y]_z^-}{R_z + [R^x]_z^+ + [R^y]_z^+} \tag{130c}$$

where

$$[R^\iota]_\kappa^+ = \begin{cases} R^\iota, & \text{if } \text{sign}(R^\iota) = \text{sign}(R^\kappa), \\ 0, & \text{otherwise,} \end{cases} \tag{131}$$

and

$$[R^\iota]_\kappa^- = \begin{cases} 0, & \text{if } \text{sign}(R^\iota) = \text{sign}(R^\kappa), \\ -R^\iota, & \text{otherwise.} \end{cases} \tag{132}$$

or

$$[R^\iota]_\kappa^- = [R^\iota]_\kappa^+ - R^\iota \tag{133}$$

where ι and κ stand for one of (though different) x, y or z each.

Then we define the following quantities

$$\begin{aligned} R^{x^*} &= R^x + \Psi(Q^y)R^y + \Psi(Q^z)R^z \\ R^{y^*} &= R^y + \Psi(Q^x)R^x + \Psi(Q^z)R^z \\ R^{z^*} &= R^z + \Psi(Q^x)R^x + \Psi(Q^y)R^y \end{aligned} \tag{134}$$

where Ψ is a non-compressive limiter.

Substituting $R^{x^*}, R^{y^*}, R^{z^*}$ into (128),(129) instead of R^x, R^y, R^z respectively we obtain a linearity preserving (second order accurate in this case) positive advection scheme.

To demonstrate this we can assume without loss of generality that

$$\begin{aligned} Q^y \cdot Q^z &\geq 0 \\ Q^x(Q^y + Q^z) &\leq 0 \end{aligned} \tag{135}$$

Then

$$\begin{aligned} Q^y &= -R^x/(R^y + R^z) \\ Q^x &\equiv 1/Q^y \\ Q^z &\equiv Q^y \end{aligned} \tag{136}$$

In this case

$$\begin{aligned} &\Psi(Q^y)R^y + \Psi(Q^z)R^z \equiv -\Psi(\tfrac{1}{Q^x})R^x \\ &\Psi(Q^x)R^x \equiv -\Psi(Q^y)(R^y + R^z) \end{aligned} \tag{137}$$

and therefore

$$\begin{aligned} R^{x^*} &= (1 - \Psi(\tfrac{1}{Q^x}))R^x \\ R^{y^*} &= (1 - \Psi(Q^y))R^y \\ R^{z^*} &= (1 - \Psi(Q^z))R^z \end{aligned} \tag{138}$$

It can be concluded that if Ψ is a non-compressive limiter, then the constructed scheme is positive.

If the fluctuation R vanishes then

$$R^x = R^y + R^z \tag{139}$$

and, therefore,

$$Q^x = Q^y = Q^z = 1. \tag{140}$$

Then it is easy to see that

$$R^{x^*} = R^{y^*} = R^{z^*} = 0, \tag{141}$$

provided $\Psi(1) = 1$, i.e. the constructed scheme is linearity preserving.

6.2. Euler system. Euler equations in three dimensions

$$\boldsymbol{u}_t + \boldsymbol{F}(\boldsymbol{u})_x + \boldsymbol{G}(\boldsymbol{u})_y + \boldsymbol{H}(\boldsymbol{u})_z = \mathbf{o} \tag{142}$$

where

$$\boldsymbol{u} = \begin{pmatrix} \rho \\ \rho u \\ \rho v \\ \rho w \\ e \end{pmatrix};$$

$$\boldsymbol{F}(\boldsymbol{u}) = \begin{pmatrix} \rho u \\ \rho u^2 + p \\ \rho uv \\ \rho uw \\ u(e+p) \end{pmatrix}; \quad \boldsymbol{G}(\boldsymbol{u}) = \begin{pmatrix} \rho v \\ \rho uv \\ \rho v^2 + p \\ \rho wv \\ v(e+p) \end{pmatrix}; \quad \boldsymbol{H}(\boldsymbol{u}) = \begin{pmatrix} \rho w \\ \rho wu \\ \rho wv \\ \rho w^2 + p \\ w(e+p) \end{pmatrix}$$

Introducing the *auxiliary* variables (s, u, v, w, p) we can rewrite these equations in the following non-conservative form

$$\begin{aligned} &s_t + us_x + vs_y + ws_z = 0 \\ &\rho u_t + \rho uu_x + \rho vu_y + \rho wu_z + p_x = 0 \\ &\rho v_t + \rho uv_x + \rho vv_y + \rho wv_z + p_y = 0 \\ &\rho w_t + \rho uw_x + \rho vw_y + \rho ww_z + p_z = 0 \\ &p_t + up_x + vp_y + wp_z + \rho c^2(u_x + v_y + w_z) = 0 \end{aligned} \tag{143}$$

Fluctuation on tetrahedron T (see Fig.5) is

$$\begin{aligned} \boldsymbol{R} = \int\int\int \boldsymbol{u}_t &= -\int\int\int (\boldsymbol{F}_x + \boldsymbol{G}_y + \boldsymbol{H}_z) dx\, dy\, dz \\ &= -V_T[\widehat{\boldsymbol{F}_x} + \widehat{\boldsymbol{G}_y} + \widehat{\boldsymbol{H}_z}] \end{aligned} \tag{144}$$

Fluctuation in *auxiliary* variables on each tetrahedron can be represented as a sum of three parts

$$\boldsymbol{r} = \boldsymbol{r}^x + \boldsymbol{r}^y + \boldsymbol{r}^z \tag{145}$$

The matrix C_a relating the fluctuations in conservative variables $\boldsymbol{R}$ to those in the auxiliary variables

$$C_a = \begin{pmatrix} 1 & 0 & 0 & 0 & 1/\tilde{c}^2 \\ \tilde{u} & 1 & 0 & 0 & \tilde{u}/\tilde{c}^2 \\ \tilde{v} & 0 & 1 & 0 & \tilde{v}/\tilde{c}^2 \\ \tilde{w} & 0 & 0 & 1 & \tilde{w}/\tilde{c}^2 \\ \tilde{U}^2/2 & \tilde{u} & \tilde{v} & \tilde{w} & 1/(\gamma-1) + \tilde{U}^2/(2\tilde{c}) \end{pmatrix} \tag{146}$$

It was pointed out in [16] that the two-dimensional conservative linearization presented there extends to three dimensions in a straightforward way. Again, we assume that the quantity that varies linearly on the tetrahedron T is the "parameter-vector" and the averaged quantities can be defined in a manner similar to the two-dimensional case. The fluctuation in the *auxiliary variables* on T can be written as follows

$$\boldsymbol{r} = -S_T \cdot \tilde{A} \cdot \boldsymbol{r}^x = -S_T \tilde{A} \cdot (\widehat{s_x}, \widehat{\rho u_x}, \widehat{\rho v_x}, \widehat{\rho w_x}, \widehat{p_x})^T \tag{147}$$

The fluctuation distribution formulae in this case are

$$\begin{aligned} V\boldsymbol{u}_1^{n+1} &= V\boldsymbol{u}_1^n + \tfrac{\tau}{2} C_a(\boldsymbol{r}^z + \bar{\boldsymbol{r}}^z) \\ V\boldsymbol{u}_2^{n+1} &= V\boldsymbol{u}_2^n + \tfrac{\tau}{2} C_a[(\boldsymbol{r}^y + \bar{\boldsymbol{r}}^y) + (\boldsymbol{r}^z - \bar{\boldsymbol{r}}^z)] \\ V\boldsymbol{u}_3^{n+1} &= V\boldsymbol{u}_3^n + \tfrac{\tau}{2} C_a[(\boldsymbol{r}^x + \bar{\boldsymbol{r}}^x) + (\boldsymbol{r}^y - \bar{\boldsymbol{r}}^y)] \\ V\boldsymbol{u}_4^{n+1} &= V\boldsymbol{u}_4^n + \tfrac{\tau}{2} C_a(\boldsymbol{r}^x - \bar{\boldsymbol{r}}^x) \end{aligned} \tag{148}$$

Similarly to the two-dimensional case, the relationship between the the artificial viscosity needed in x-direction to obtain the upwind scheme and $\boldsymbol{r}^x$ is the following

$$\bar{\boldsymbol{r}}^x = \text{sign}(\tilde{A})\boldsymbol{r}^x. \tag{149}$$

$\bar{\boldsymbol{r}}^y$ and $\bar{\boldsymbol{r}}^z$ can be evaluated in a similar way.

Denoting

$$M_x = \text{sign}(\tilde{A})$$

it can be verified that

$$M_x = \begin{cases} M_x^{sub}, & \text{if } |\tilde{u}| \le \tilde{c} \\ M_x^{sup}, & \text{if } |\tilde{u}| > \tilde{c}, \end{cases} \tag{150}$$

where

$$M_x^{sub} = \begin{pmatrix} \text{sign}(\tilde{u}) & 0 & 0 & 0 & 0 \\ 0 & 0 & 0 & 0 & 1/\tilde{c} \\ 0 & 0 & \text{sign}(\tilde{u}) & 0 & 0 \\ 0 & 0 & 0 & \text{sign}(\tilde{u}) & 0 \\ 0 & \tilde{c} & 0 & 0 & 0 \end{pmatrix} \tag{151}$$

and

$$M_x^{sup} = \text{sign}(\tilde{u})I \tag{152}$$

Following the procedure of constructing a high resolution scalar advection scheme in three dimensions, presented briefly in §6.1 we define the following quantities

$$q_i^x = \frac{[r_i^y]_x^- + [r_i^z]_x^-}{r_i^x + [r_i^y]_x^+ + [r_i^z]_x^+} \tag{153}$$

$$q_i^y = \frac{[r_i^x]_y^- + [r_i^z]_y^-}{r_i^y + [r_i^x]_y^+ + [r_i^z]_y^+} \tag{154}$$

$$q_i^z = \frac{[r_i^x]_z^- + [r_i^y]_z^-}{r_i^z + [r_i^x]_z^+ + [r_i^y]_z^+} \tag{155}$$

where $[\ldots]_x^{\pm}, [\ldots]_y^{\pm}, [\ldots]_z^{\pm}$ are defined by (131),(132). Now we can introduce

$$\begin{aligned} r_i^{x^*} &= r_i^x + \Psi(q_i^y) r_i^y + \Psi(q_i^z) r_i^z \\ r_i^{y^*} &= r_i^y + \Psi(q_i^x) r_i^x + \Psi(q_i^z) r_i^z \\ r_i^{z^*} &= r_i^z + \Psi(q_i^x) r_i^x + \Psi(q_i^y) r_i^y \end{aligned} \tag{156}$$

for $i = 1, ..., 5$.

Substituting $\boldsymbol{r}^{x^*}, \boldsymbol{r}^{y^*}, \boldsymbol{r}^{z^*}$ instead of $\boldsymbol{r}^x, \boldsymbol{r}^y, \boldsymbol{r}^z$ into the fluctuation distribution formulae (148) and (149) we obtain a linearity preserving (second order accurate for the case of structured meshes) genuinely three-dimensional scheme for the Euler equations.

Note that

$$\boldsymbol{r} \equiv \boldsymbol{r}^x + \boldsymbol{r}^y + \boldsymbol{r}^z \equiv \boldsymbol{r}^{x^*} + \boldsymbol{r}^{y^*} + \boldsymbol{r}^{z^*}. \tag{157}$$

Therefore, the constructed scheme is conservative. It is also easy to see that it is linearity preserving.

7. Multigrid solver. One of the most attractive properties of the constructed multidimensional scheme for the Euler equations is that the Collective Gauss-Seidel relaxation is stable when applied directly to the high-resolution discrete equations. This can be utilized to construct a very simple and efficient steady-state multigrid solver. In this work we would like just to illustrate the basic advantages of the multigrid solver that uses the constructed multidimensional scheme. Therefore, we do not discuss here any issues concerning the multigrid algorithm for general unstructured meshes, but address the interested reader to the literature (see, for instance, [11]).

We shall present briefly in this section the simple multigrid algorithm used in the numerical experiments presented in this work.

Description of the algorithm. The multigrid cycle used in this work is W-cycle and the entire algorithm can be implemented either as *Cycling* or as *Full Multigrid* (FMG).

Relaxation. The algorithm employs the Collective Gauss-Seidel relaxation as a smoother. In order to update the solution at each node a system of four nonlinear equations has to be solved. This can be done using the Newton method. One iteration at each node is sufficient for this purpose (see [18] for the discussion on this matter). The ordering of the relaxation can be Red-Black, lexicographic etc.

Restriction and prolongation. Assume that we have a hierarchical sequence of triangular grids, i.e. that any triangle on the coarser grid is a union of four triangles on the finer grid. The natural choice for prolongation in this case would be a linear interpolation along each face of the triangle belonging to the coarser grid. The restriction in this case can be just combining the fluctuations from the four finer grid triangles forming the coarse grid one. However, we consider only Cartesian grids in the numerical experiments presented in this work (see Figs.2,3). In this case we can use more conventional prolongation and restriction operators: bilinear correction interpolation and Full-Weighting of the residuals (see [1]). Term "residual" is used here in its usual sense: residual of the discrete equation at each gridpoint (constructed from the contributions from the triangles having this gridpoint as a common vertex).

Previous relevant results. Application of multigrid methods for the advection equation was studied in detail in [17],[18] in conjunction with the genuinely two-dimensional control-volume type scheme developed there. It was demonstrated there that applying the $2FMG - W(2,1)$ algorithm is sufficient to obtain high quality solutions (i.e. solutions with sharply resolved discontinuities and second order accuracy both in smooth regions and in discontinuity location) for the advection equation. Many of the conclusions of [17],[18] apply directly to the Euler system case considered in this work.

Efficiency of the multigrid solver for advection-dominated problems. It was shown in [1] that the residual reduction per multigrid cycle for an advection (dominated) problem cannot in general be better than .75 for the second order accurate discretization (.5 for the first order). This is because the coarse grid provides only a fraction (.75 or .5 respectively) of the needed correction for some components. The ability of the multigrid algorithm to achieve a rate of convergence close to .75 (for the second order accurate approximation) means that the obstacle towards achieving a better efficiency are not the smoothing properties of the relaxation but rather an insufficient coarse grid correction for certain components. (see §9.2.2 for further discussion on this issue).

8. Numerical experiments. The purpose of the numerical experiments reported in this section is to verify the robustness of the constructed scheme and the quality of the numerical solutions obtained by its means. Some preliminary experiments illustrating the performance of the multigrid algorithm uzing this scheme are presented as well.

8.1. Supersonic flow in a channel with a bump. The test case considered here is a supersonic (Mach=2.9) flow in channel with a circular bump. The bump is located at the lower wall of the channel at $1 \leq x \leq 2.$ and its surface is a circular arch of $\pi/3$ and radius 1. Note that the actual shape of the domain is a rectangle. The

influence of the bump on the flow is imposed through the boundary conditions: the velocity component normal to the surface of the bump at a certain location is being reflected.

The first experiment uses a grid of size 200×40 points. The density contour plots of the steady-state solution are presented on Fig.6(a). The scheme used is the one given by (71),(72), (73) in §4 with the *minmod* limiter.

The second experiment presented in Fig.6(b) corresponds to the same settings, except that the grid is twice finer (400×80 points). As it is expected, the grid refinement results in a better resolution of the flow features.

The third experiment (Fig.6(c)) is performed on the grid of the same size as the first one. However, the triangulation is as illustrated on Fig.3 and the scheme employed is constructed according to (115),(116),(123) in §5 and the derivatives are approximated using the diagonal and parallel to the x direction faces of the triangles. Even though the grid is structured, the most essential feature of the unstructured grid formulation of the scheme - use of the non-orthogonal coordinate system is present.

The purpose of this experiment is to test the performance of such a scheme and to illustrate the effect of the scheme and triangulation on the resolution of discontinuities. It can be seen in Fig.6(c) that the shock reflected from the upper wall is resolved better than the stronger one that is incident to the upper wall. This is because for this scheme/grid combination, discontinuities whose direction is close to the grid diagonal (upper-left to lower-right) will be resolved very well (in addition to those which are close to the horizontal or vertical directions).

8.2. Transonic flow over a circular bump. The testcase considered here is a transonic flow (free-stream Mach= .9) over a flat wall with a bump (Fig.7). The surface of the bump is a circular arch of $\pi/3$ and radius 1 and its location is between $3.5 \leq x \leq 4.5$. Again, in order to keep the experiments simple at this stage of work, the bump is treated the same way as in the previous experiments. The grid is 200×200 points and the scheme used is presented in §4. The shock of the "fish-tail" shape can be clearly observed in Fig.7.

8.3. Low Mach number flow over a circular bump. Here we present a numerical experiment concerning a low Mach number (=.1) flow over a flat wall with a circular (arch of $\pi/3$ and radius 2) bump. Here as well as in the previous case the presence of the bump is imitated through the appropriate boundary conditions. The grid is 200×200 points. The density contours of the steady-state solution are presented in Fig.8.

8.4. Multigrid algorithm. To illustrate the performance of the multigrid algorithm we consider here the well known testcase of a shock reflecting from a flat wall. The multigrid algorithm involves five grids (levels): the finest consists of 129×33 points, the coarsest is 9×3 points.

The multigrid algorithm is based on the scheme presented in §4 used with the lexicographic Gauss-Seidel relaxation. The restriction and prolongation procedures are the standard Full Weighting of the residuals and bilinear correction interpolation. The first experiment performs one $W(2,1)$ cycle. Fig.9(a) presents the initial guess and Fig.9(b) – the numerical solution obtained by one $W(2,1)$ cycle. It is remarkable that such little computational work is sufficient to make the reflected shock clearly visible. The numerical solution to this problem obtained by the $2FMG - W(2,1)$

algorithm is presented on Fig.9(c).

Note that in this case the flow is aligned with the x-direction in a significant part of the domain. In this case the artificial viscosity in the cross-stream direction in the entropy and u-momentum equations (see §4) vanishes. Therefore, no smoothing can be obtained in the y-direction in some components. A multigrid algorithm utilizing the time-stepping type relaxation can deal with such a situation only using the semi-coarsening technique. Our algorithm employs the Gauss-Seidel relaxation. Therefore, it offers a much simpler and more efficient treatment of this problem: relaxation with lexicographic ordering in the stream direction.

The rate of convergence observed in this testcase as well as in other simple experiments concerning a variety of flow regimes is very close to .75 (see §§7,9.2.2 for a discussion).

9. Discussion and conclusions.

9.1. Summary of the current work. A new two-dimensional high-resolution (at the steady-state) scheme for the compressible Euler equations was presented. It is triangle-based and can be formulated with the same degree of simplicity both on structured and unstructured grids. The main advantage of this scheme is that Gauss-Seidel relaxation can be applied directly to the resulting discrete equations. This allows construction of a simple and efficient multigrid steady-state solver.

A remarkable property of the constructed scheme is also its very compact stencil: it involves only the immediate neighbors of the point of interest.

A variety of flow regimes (supersonic, transonic and low Mach number flow) were considered in the numerical experiments to verify the quality of the solutions obtained by means of the new scheme and to demonstrate the efficiency of the multigrid algorithm.

Generalization of this scheme to three dimensional tetrahedral meshes is presented briefly as well.

9.2. Future work.

9.2.1. Compressible Navier-Stokes equations. The extension of this scheme to the case of the compressible Navier-Stokes equations is straightforward. It is interesting to note that the artificial viscosity present in the momentum equations in the subsonic case contains already terms of the type $(u_x + v_y)_x$ and $(u_x + v_y)_y$ that appear in the physical viscosity of the compressible Navier-Stokes equations.

9.2.2. Further improvement of the multigrid efficiency. As it was mentioned in §7 the main obstacle towards the further improvement of the multigrid efficiency is the following fact: for the hyperbolic problems the coarse grid correction is not sufficient for certain error components.

This difficulty was already addressed in the literature and some techniques to improve the multigrid efficiency were developed in [2]. Therefore, one possibility is to adapt these techniques for our case - compressible Euler equations.

We shall mention here another way to deal with this difficulty. The steady-state compressible Euler equations in the subsonic case are very similar from the mathematical point of view to the incompressible Euler equations – both problems are of the mixed elliptic-hyperbolic type.

There exist very efficient steady-state multigrid solvers for the incompressible flow equations, which rely on the primitive variables formulation (velocities and pressure). Most of them employ staggered grid discretization of the equations. A typical efficiency of such algorithms for a low Reynolds number case is comparable to that for the Poisson equation. However, the convergence rate deteriorates for the advection dominated (high Reynolds number) flow. Typical numerical schemes for incompressible flow are constructed in such a way that a certain "separation" of the elliptic and hyperbolic (advection) factors of the equations is achieved in this case (see [1]). Assume that the flow structure is simple enough (i.e. there is no recirculation, etc.), and it is possible to perform relaxation in the stream direction. Then one can still recover the optimal efficiency efficiency of the multigrid solver (see [25]).

However, constructing a discretization that achieves a similar separation of the advection and "full-potential" factors of the compressible Euler equations appeared to be a very difficult problem despite the similarity of the steady-state equations for compressible and incompressible cases. A canonical variable formulation of the Euler equations for both cases was suggested recently by Ta'asan [23]. This formulation facilitated the construction of the discrete scheme (using staggered grids) and of the relaxation procedure that separate a treatment of the advection and full-potential factors (see [24]). The resulting multigrid algorithm achieves a very good efficiency (the same as for the full-potential equation) in the subsonic case provided it is possible to perform relaxation in the flow direction.

One of the future possible directions is to modify the scheme presented in this work so that it will achieve a similar efficiency for the case of triangular (non-staggered and, possibly, unstructured) grids. This is possible because some very important similarities between the present scheme and the existing discretizations for the incompressible flow equations used in very efficient multigrid solvers (see, for instance, [1]) can be observed (see §9.3). The resulting discretization will rely on the primitive rather then the canonical variables. The latter is crucial for the further generalization of the solver to the compressible Navier-Stokes equations.

9.2.3. Time-dependent problems. The constructed scheme is capable of producing high-resolution (second order accurate on the structured grids) steady-state solutions for the compressible Euler equations. A very natural way to extend this capability to the transient problems is to use a Lax-Wendroff type modification of the constructed scheme, i.e. to scale the artificial viscosity in such a way that it will cancel the time error of the forward Euler time-stepping due to the equation (or system of equations) being solved.

To illustrate this on the simple case of the two-dimensional advection consider the scheme for the structured grids presented in §2.1.2. The use of the following artificial viscosity

$$\begin{aligned} \bar{R}^x &= \tfrac{\tau}{h} a R^x \\ \bar{R}^y &= \tfrac{\tau}{h} b R^y. \end{aligned} \tag{158}$$

instead of the one given by (5) results in a high-resolution scheme (constructed by substituting R^{x^*}, R^{y^*} defined by (6) instead of R^x, R^y) that is second order accurate in time and space. However, it is easy to see that in general this scheme is not of the positive type anymore (see also [6]).

For the case of the Euler system, modifying the construction of the high-resolution scheme presented in §4 by substituting the artificial viscosity defined as follows

$$\bar{r}^x = \frac{\tau}{h}\tilde{A}r^x \qquad \bar{r}^y = \frac{\tau}{h}\tilde{B}r^y \tag{159}$$

instead of (72), results in a Lax-Wendroff type scheme. However, the applicability of this scheme is restricted to problems with no strong shocks.

It is interesting to note that the two-dimensional schemes by Colella [3],[4], LeVeque [10], Radvogin [12] can be interpreted as schemes of the Lax-Wendroff type. However, the nonlinear mechanism that enables them to deal with (strong) shocks relies on one-dimensional limiters and characteristic variables in the x and y direction, which introduces an essential flavor of dimensional splitting.

The first step towards the construction of a genuinely multidimensional time-space accurate and robust Euler scheme should be to construct a positive time-space accurate scalar advection scheme of the type Lax-Wendroff type. This is one of the directions currently being investigated.

9.3. What is a truly multidimensional scheme ?. Perhaps, it will be easier to answer this question after the nonoscillatory time-space accurate multidimensional scheme for the compressible Euler equations is constructed. However, some attributes of the truly multidimensional schemes can be seen already in the scheme constructed here.

One of the main characteristics of a truly multidimensional scheme for fluid dynamics is that a multidimensional operator such as the divergence operator (present in the pressure equation, the auxiliary variables formulation of the Euler system (56)) should be represented in a difference scheme as whole. This is not the case for the dimensionally split schemes. It can be clearly seen in the example of the dimensional upwinding scheme (71),(72) that terms u_x and v_y are separated (when contributing to the artificial viscosity of the momentum and pressure equations).

Consider the case of subsonic flow. In this case the fluctuation of the pressure equation contributes to the artificial diffusion of the momentum equations. Let us modify slightly the scheme constructed in §4 and compute the fluctuation of the pressure equation contributing to the artificial viscosity terms of the momentum equations according to the following

$$r_4^{x^*} \equiv r_4^{y^*} = r_4^x + r_4^y. \tag{160}$$

The only difference between (160) and (73) is that the limiter function is set to unity. Although

$$r_4^{x^*} + r_4^{y^*} = 2r_4 \neq r_4,$$

such a scheme is conservative, since (160) is used only in the artificial viscosity. This is because the role of the artificial viscosity can be interpreted as "redistribution" of the fluctuations split by the central scheme - to subtract a certain amount from one vertex of the triangle and to add the same amount to another vertex. This does not violate conservation, regardless of what amount has been "redistributed".

Recall, that for some very popular schemes for incompressible flow (see, for instance, [1]) the residual of the continuity equation contributes to the velocities update in such a way that the discrete vorticity remains unchanged.

The "physical" meaning of this is that the change in (evolution of) the vorticity is only due to the residuals of the momentum equations, as one would expect. The "mathematical" meaning of this fact is that the elliptic factor of the incompressible Euler equations is being discretized and relaxed as such. This allowed construction of a highly efficient multigrid solver (see [1]).

What can be observed clearly in the subsonic case is that the fluctuation of the pressure equation (being a part of artificial diffusion of the discretized momentum equations) contributes to the change of the velocities (divergence update) according to exactly the same pattern as the residual of the continuity equation in the schemes for discretizing the equations of incompressible flow.

Thus, the scheme presented in this work establishes a link between some standard techniques used for solving equations of the incompressible flow and the class of upwind schemes commonly used for compressible flow computations.

Acknowledgments. The author would like to express his gratitude to Marsha Berger, Jonathan Goodman and Peter Lax for numerous stimulating discussions, and for making his stay at the Courant Institute such an enchanting experience.

The author would also like to thank Philip Roe for valuable discussions, particularly of the three-dimensional advection, and for his cheerful and encouraging attitude. Finally, the author is grateful to Ken Powell and Bram van Leer for their continuing interest in this work.

REFERENCES

[1] A. BRANDT, *Multigrid techniques: 1984 guide with applications to fluid dynamics*, The Weizmann Institute of Science, Rehovot, Israel, 1984.

[2] A. BRANDT AND I. YAVNEH, *Accelerated multigrid convergence and high reynolds recirculating flows*, SISC, 14 (1993), pp. 607–626.

[3] P. COLELLA, *Multidimensional upwind methods for hyperbolic conservation laws*, Tech. Rep. LBL-17023, Lawrence Berkeley Report, 1984.

[4] ——, *Multidimensional upwind methods for hyperbolic conservation laws*, JCP, 87 (1990), p. 171.

[5] H. DECONINCK, C. HIRSCH, AND J. PEUTEMAN, *Characteristic decomposition methods for for the multidimensional euler equations*, in Lecture Notes in Physics 264, Springer, 1986, pp. 216–221.

[6] H. DECONINCK, R. STRUIJS, AND P. L. ROE, *Fluctuation splitting for multidimensional convection problem: an alternative to finite volume and finite element methods*, vki lecture series 1990-3 on computational fluid dynamics, Von Karman Institute, Brussels, Belgium, mar 1991.

[7] A. JAMESON, *Transonic airfoil calculations using the euler equations*, in Numerical Methods in Aeronautical Fluid Dynamics., P. L. Roe, ed., Academic Press, New York, 1982.

[8] ——, *Solution of the euler equations for two dimensional transonic flow by a multigrid method*, Applied Math. and Computation, 13 (1983), pp. 327–355.

[9] A. JAMESON, W. SCHMIDT, AND E. TURKEL, *Numerical simulation of the euler equations by finite volume method using runge-kutta time-stepping schemes*, AIAA Paper 81-1259, AIAA 5th Computational Fluid Dynamics Conference., 1981.

[10] R. J. LEVEQUE, *High resolution finite volume methods on arbitrary grids via wave propagation*, JCP, 78 (1988).

[11] D. J. MAVRIPLIS, *Multigrid solution of the two-dimensional euler equations on unstructured triangular meshes*, AIAA Journal, 26 (1988), pp. 824–831.

[12] Y. B. RADVOGIN, *Quasi-monotonous multidimensional difference schemes with second order accuracy*. Soviet Academy of Science Preprint, 1991.

[13] P. L. ROE, *Approximate riemann solvers, parameter vectors, and difference schemes*, JCP, 43 (1981), pp. 357–372.

[14] ——, *Discrete models for the numerical analysis of time-dependent multidimensional gas dynamics*, JCP, 63 (1986), pp. 458–476.

[15] ——, *Discontinuous solutions to hyperbolic systems under operator splitting*, Tech. Rep. Report No. 87-64, ICASE, 1987.

[16] P. L. ROE, R. STRUIJS, AND H. DECONINCK, *A conservative linearization of the multidimensional Euler equations*. To appear in J. Comp. Phys.

[17] D. SIDILKOVER, *Numerical solution to steady-state problems with discontinuities*, PhD thesis, The Weizmann institute of Science, Rehovot, Israel, 1989.

[18] D. SIDILKOVER AND A. BRANDT, *Multigrid solution to steady-state 2d conservation laws*, SINUM, 30 (1993), pp. 249–274.

[19] D. SIDILKOVER AND P. L. ROE, *Unification of some advection schemes in two dimensions*. Submitted to Math. Comp.

[20] S. SPEKREIJSE, *Multigrid solution of monotone second-order discretization of hyperbolic conservation laws*, Math. Comp., 49 (1987), pp. 135–155.

[21] ——, *Multigrid solution of the steady Euler equations*, PhD thesis, CWI, Amsterdam, 1987.

[22] R. STRUIJS, H. DECONINCK, P. DE PALMA, P. L. ROE, AND K. G. POWELL, *Progress on multidimensional upwind euler solvers for unstructured grids*. AIAA 91-1550, June 24-26 1991. Honolulu, Hawai.

[23] S. TA'ASAN, *Canonical forms of multidimensional steady inviscid flows*, Report No. 93-94, ICASE, 1993.

[24] ——, *Canonical-variables multigrid method for steady-state euler equations*, Report No. 94-14, ICASE, 1994.

[25] I. YAVNEH, *Multigrid Techniques for Incompressible Flows*, PhD thesis, Weizmann Institute of Science, Rehovot, Israel, 1991.

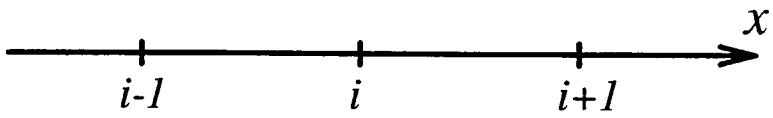

FIG. 1. *One-dimensional grid.*

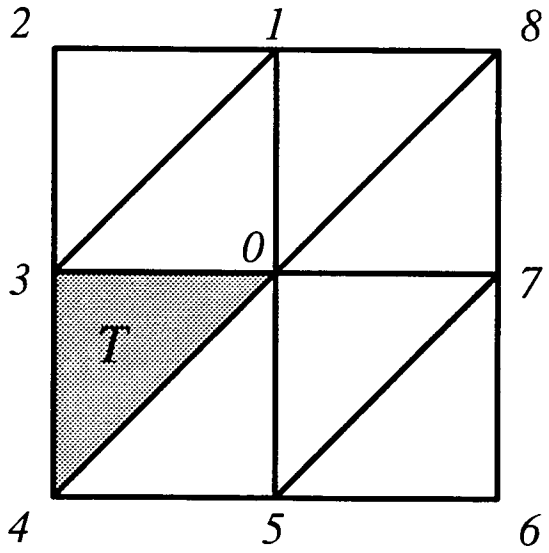

FIG. 2. *Triangulation I.*

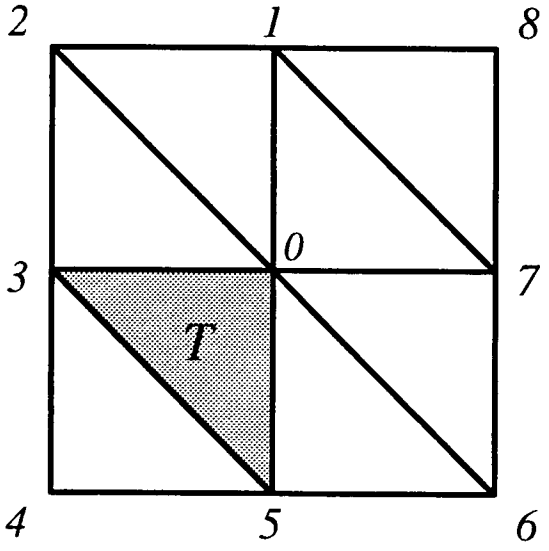

FIG. 3. *Triangulation II.*

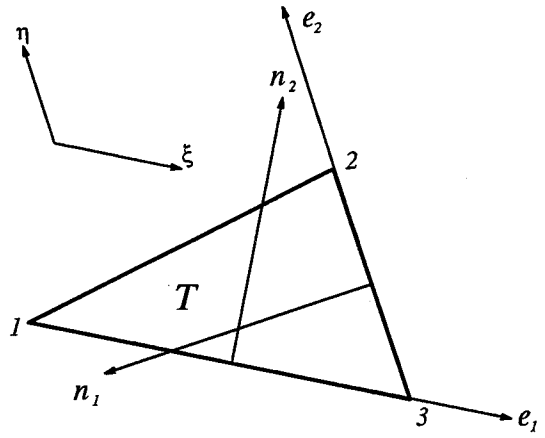

FIG. 4. *Triangle.*

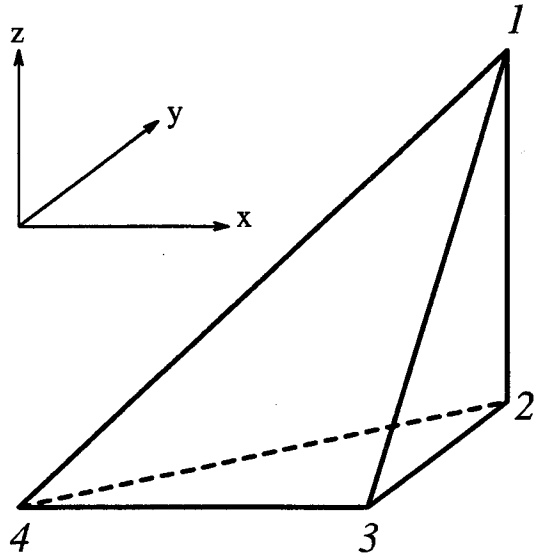

FIG. 5. *Tetrahedron.*

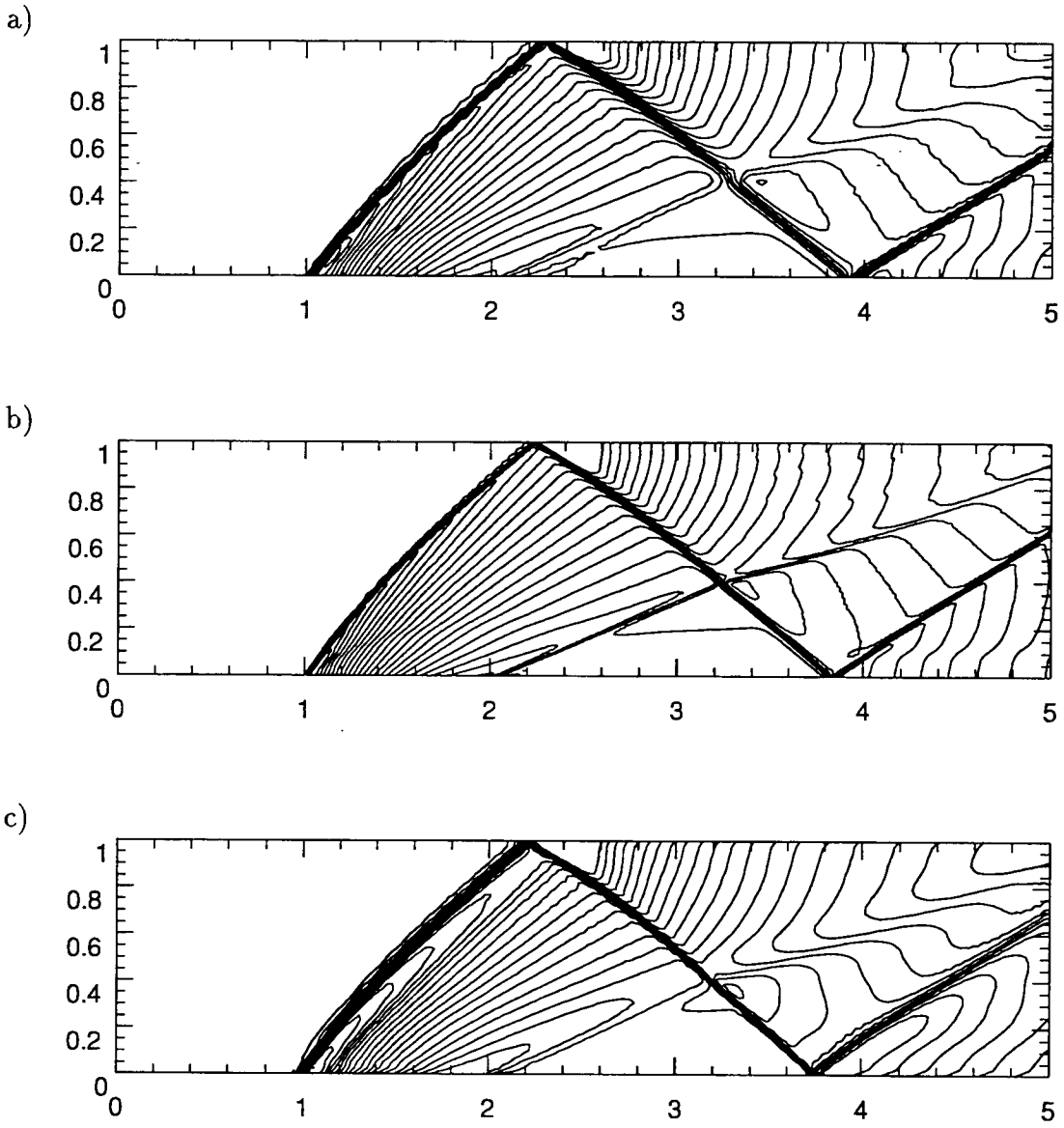

FIG. 6. *Supersonic flow in a channel over a circular bump: a) grid* 200×40 *pts., triangulation I, scheme from §4; b) the same, except the grid* 400×80 *pts.; c) grid* 200×40 *pts., triangulation II, scheme according to §5, which relies on the approximate derivatives along the nonorthogonal faces of the triangles.*

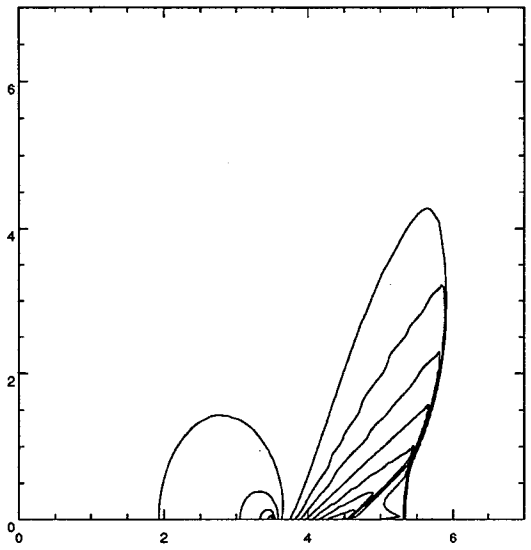

FIG. 7. *Transonic flow over a wall with a circular bump (free stream Mach= .9).*

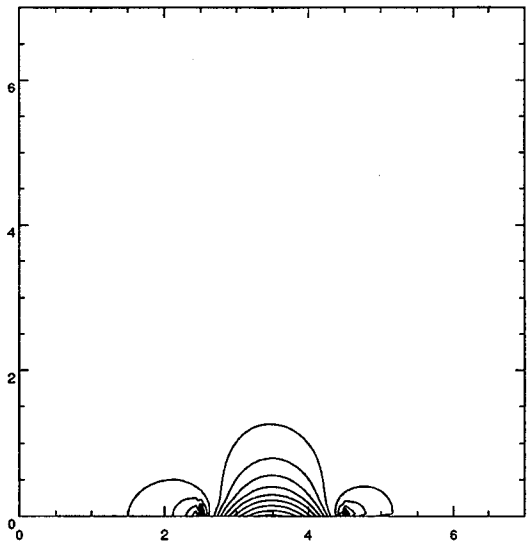

FIG. 8. *Low speed flow (Mach= .1) over a wall with a circular bump.*

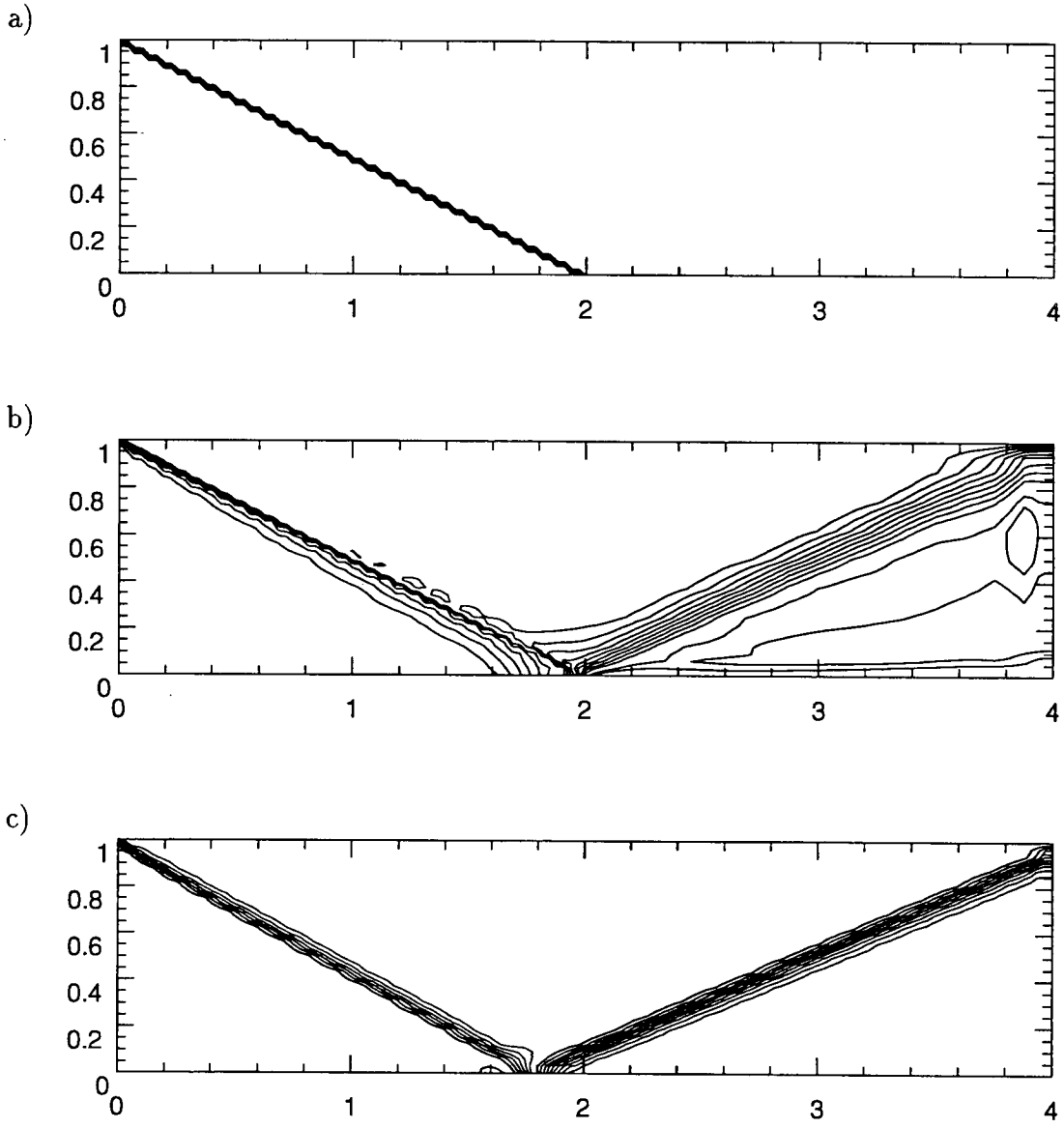

FIG. 9. *Performance of the multigrid algorithm, grid* 129×33 *pts.: a) initial guess; b) result of applying one* $W(2,1)$ *cycle; c) solution obtained by* $2FMG - W(2,1)$ *algorithm.*

REPORT DOCUMENTATION PAGE

Form Approved
OMB No. 0704-0188

1. AGENCY USE ONLY *(Leave blank)*	2. REPORT DATE	3. REPORT TYPE AND DATES COVERED
	November 1994	Contractor Report

4. TITLE AND SUBTITLE
A GENUINELY MULTIDIMENSIONAL UPWIND SCHEME AND EFFICIENT MULTIGRID SOLVER FOR THE COMPRESSIBLE EULER EQUATIONS

5. FUNDING NUMBERS
C NAS1-19480
WU 505-90-52-01

6. AUTHOR(S)
David Sidilkover

7. PERFORMING ORGANIZATION NAME(S) AND ADDRESS(ES)
Institute for Computer Applications in Science
and Engineering
Mail Stop 132C, NASA Langley Research Center
Hampton, VA 23681-0001

8. PERFORMING ORGANIZATION REPORT NUMBER
ICASE Report No. 94-84

9. SPONSORING/MONITORING AGENCY NAME(S) AND ADDRESS(ES)
National Aeronautics and Space Administration
Langley Research Center
Hampton, VA 23681-0001

10. SPONSORING/MONITORING AGENCY REPORT NUMBER
NASA CR-195000
ICASE Report No. 94-84

11. SUPPLEMENTARY NOTES
Langley Technical Monitor: Michael F. Card
Final Report
To be submitted to the Journal of Computational Physics

12a. DISTRIBUTION/AVAILABILITY STATEMENT
Unclassified–Unlimited

Subject Category 64

12b. DISTRIBUTION CODE

13. ABSTRACT *(Maximum 200 words)*

We present a new approach towards the construction of a genuinely multidimensional high-resolution scheme for computing steady-state solutions of the Euler equations of gas dynamics. The unique advantage of this approach is that the Gauss-Seidel relaxation is stable when applied directly to the high-resolution discrete equations, thus allowing us to construct a very efficient and simple multigrid steady-state solver. This is the only high-resolution scheme known to us that has this property. The two-dimensional scheme is presented in detail. It is formulated on triangular (structured and unstructured) meshes and can be interpreted as a genuinely two-dimensional extension of the Roe scheme. The quality of the solutions obtained using this scheme and the performance of the multigrid algorithm are illustrated by the numerical experiments. Construction of the three-dimensional scheme is outlined briefly as well.

14. SUBJECT TERMS
genuinely multidimensional scheme; compressible flow; steady-state solutions; multigrid methods

15. NUMBER OF PAGES
36

16. PRICE CODE
A03

17. SECURITY CLASSIFICATION OF REPORT	18. SECURITY CLASSIFICATION OF THIS PAGE	19. SECURITY CLASSIFICATION OF ABSTRACT	20. LIMITATION OF ABSTRACT
Unclassified	Unclassified		